Hybrid Simulation 101 Short Course
NHERI Lehigh Experimental Facility
Lehigh University
June 24, 2025

Hybrid Simulation 101: Short course on the Theory, Implementation, and Application of Real-time Hybrid Simulation

James Ricles, Ph.D., P.E.
Bruce G. Johnston Professor
Director, NHERI Lehigh Real-time Multi-Directional Hybrid Simulation Facility
Director, ATLSS Engineering Research Center

Faisal Nissar Malik
PhD Graduate Research Assistant,
NHERI Lehigh Real-time Multi-Directional Hybrid Simulation Facility

Lehigh University

Hybrid Simulation Short Course Syllabus

Short course Objectives

This short course provides a comprehensive overview of the various aspects of hybrid simulation. The participants are given the assignment to apply the method to assess the seismic performance and resiliency of a structural system. The objectives of the course are:

1) Gain foundational knowledge about hybrid simulation and its applications.
2) Acquire hands-on experience by participating in an exercise involving real-time hybrid simulation.
3) Create an awareness and appreciation of the power of using real-time hybrid simulation to assess the performance of complex systems subjected to extreme natural hazards.

Course Contents

1) Session 1: Overview and Motivation for Using Hybrid Simulation
2) Session 2: Hybrid Simulation Background and Theory
3) Session 3: Implementation and Execution to Perform a Real-time Hybrid Simulation (RTHS)
4) Session 4: Hands-on RTHS Group Assignment
5) Session 5: Short course - Perform RTHS
6) Session 6: Group Presentations of RTHS Outcomes and Conclusions

Hybrid Simulation Short Course Syllabus

Workshop References

1) Course Notes (QR code to be posted)
2) List RTHS References (QR code to be posted)

Prerequisites

The workshop is a short course on the theory and implementation of hybrid simulation, and its application to structural systems subjected to extreme natural hazards. The emphasis will be on real-time hybrid simulation (RTHS). Hybrid simulation involves the need to integrate theories from across several different disciplines. These include structural analysis, structural dynamics, structural mechanics, control engineering, numerical methods, linear algebra, computer science, artificial intelligence, and machine learning. While participants are likely not to have a familiarity with all of these theories, they can enhance their understanding of hybrid simulation by studying the course notes and reading the references.

Assignments

Participants will be divided into groups. Each group will be using RTHS to assess the seismic performance of a structural steel building system. A presentation will be made by each group, where they present their simulation outcomes, an assessment, and conclusions.

Short Course Assignment

Evaluate the seismic performance of the Lateral Force Resisting System (LFRS) for the structure shown below

- What is the efficacy of the dampers?
- What are the effects of the soil-foundation-structure interaction?
- What is the performance under two prescribed hazard levels –
  - Design Basis Earthquake (DBE – 474-year return period)
  - Maximum Considered Earthquake (MCE – 2474-year return period)

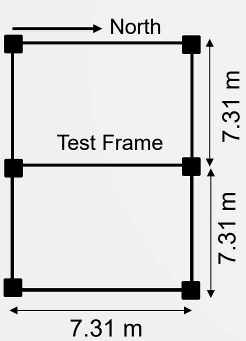

Floor Plan

- W12X45 beams
- W14X43 columns

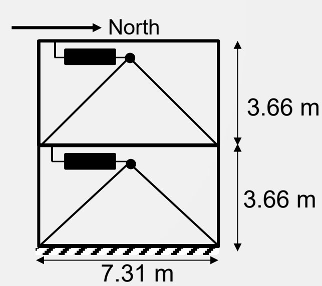

Elevation

Short Course Assignment

- W12X45 beams and W14X43 columns
- 3D force-based fiber beam column elements
  - BelPlastic Material as uniaxial material in the fibers
  - 5-point Lobatto integration scheme
- P-Delta effects accounted for by using lean on P-Delta columns
- Gravity loading
  - 413.34 kN on the first floor
  - 411.28 kN on the second floor
- Building located in Pomona California on a stiff soil (Type D)
- Two levels of hazard considered
  - DBE (474 years return period)
  - MCE (2474 years return period)
- Friction dampers in the first and second story

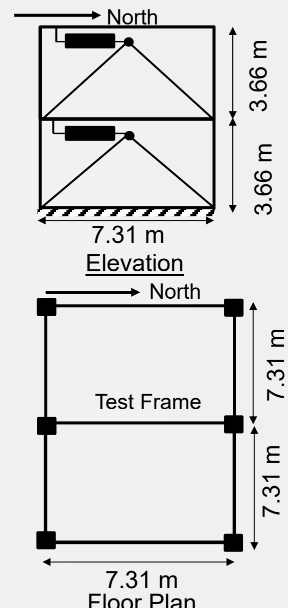

Short Course Assignment

- A HyCoM-3D input file and manual are provided on Workstations in Life Cycle Computational Lab
- The file needs to be completed by each individual group
  - Compare the natural periods obtained from the eigenvalue analysis
- A total of 6 cases need to be run
  - Without dampers (Will be done in Life Cycle Computational Lab)
    - DBE and MCE
  - With dampers on a fixed foundation (RTHS – Will be done in the control room)
    - DBE and MCE
  - With dampers considering SFSI (RTHS – Will be done in the control room)
    - DBE and MCE
- Each group will be assigned a workstation and will have to complete the HyCoM-3D input file and run the cases without dampers for the two specified hazard levels
  - Compare the results obtained from your analysis to the provided results

Hybrid Simulation Short Course References

Hybrid Simulation Shortcourse
NHERI Lehigh Experimental Facility
Lehigh University
June 24, 2025

Hybrid Simulation List of Refeered Journal References
of
James Michael Ricles, Ph.D., P.E.

1. Zhang. Y., Sause, R., Ricles, J., and C. Naito, "Modified Predictor-Corrector Numerical Scheme for Real-Time Pseudo Dynamic Testing Using State-Space Formulation," *Earthquake Engineering and Structural Dynamics*, 34(3), pp. 271-288, 2005.
2. Mercan, O. Y. and J. M. Ricles, "Stability and Accuracy Analysis of Outer Loop Dynamics in Real-Time Pseudo-Dynamic Testing of SDOF Systems," *Earthquake Engineering and Structural Dynamics*, Vol. 36(11), pp. 1523-1543, 2007.
3. Chen, C. and J.M. Ricles, "Development of Direct Integration Algorithms for Structural Dynamics using Discrete Control Theory," *Journal of Engineering Mechanics*, ASCE, Vol. 134(8), pp. 676-683, 2008.
4. Chen ,C. and J.M. Ricles, "Stability Analysis of Direct Integration Algorithms Applied to Nonlinear Structural Dynamics," *Journal of Engineering Mechanics*, ASCE, Vol. 134(9), pp. 703-711, 2008.
5. Chen, C., and J.M. Ricles, "Stability Analysis of SDOF Real-Time Hybrid Testing Systems with Explicit Integration Algorithms and Actuator Delay," *Earthquake Engineering and Structural Dynamics*, Vol 37(4), pp. 597-613, 2008.
6. Mercan, O., Ricles, J.M., Sause, R. and T. Marullo, "Real-Time Large-Scale Hybrid Testing for Seismic Performance Evaluation of Smart Structures," *International Journal for Smart Structures and Systems*, Vol. 4(5), pp. 667-684, 2008.
7. Mercan, O. and Ricles, J.M., "Stability Analysis for Real-time Pseudodynamic and Hybrid Pseudodynamic Testing With Multiple Sources of Delay," Earthquake Engineering and Structural Dynamics, Vol. 37(10), pp. 1269-1293, 2008.
8. Mercan, O. and Ricles, J.M., "Experimental Studies on Real-time Testing of Structures with Elastomeric Dampers," *Journal of Structural Engineering*, ASCE, Vol. 135(9), pp. 1124–1133, 2009.
9. Mercan, O, Ricles, J.M., Sause, R, and T. Marullo, "Kinematic Transformations in Planar Multi-directional Pseudo-Dynamic Testing," Earthquake Engineering and Structural Dynamics, Vol. 38(9), pp. 1093-1119, https://doi.org/10.1002/eqe.886, 2009.
10. Chen, C., Ricles, J.M., Marullo, T., and O. Mercan "Real-Time Hybrid Testing using the Unconditionally Stable Explicit CR Integration Algorithm," Earthquake Engineering and Structural Dynamics, Vol 38(1), pp. 23-44, https://doi.org/10.1002/eqe.838, 2009.

1 of 7

. . .

Hybrid Simulation Shortcourse
NHERI Lehigh Experimental Facility
Lehigh University
June 24, 2025

62. Dong, B., and Ricles, J.M. "Towards seismic performance quantification of viscous damped steel structure: Site-specific hazard analysis and response prediction," *Engineering Structures*, 280 (2023), 115677, https://doi.org/10.1016/j.engstruct.2023.115677, 2023.
63. Al-Subaihawi, S., Ricles, J., Quiel, S. and T. Marullo. "Unconditionally Stable Central Difference Dissipative Algorithm for Multi-directional Real-Time Hybrid Simulations of Large Nonlinear Structural Systems," *Journal of Earthquake Engineering*, 28(11), 3256-3290, http://doe.org/10.1080/13632469.2024.2333822, 2024.
64. Al-Subaihawi, S., Ricles, J., Abu-Kassab, Q., Suleiman, M., Sause, R., and T. Marullo. "Coupled Aero-Hydro-Geotech Real-Time Hybrid Simulation of Offshore Wind Turbine Monopile Structures," *Journal of Engineering Structures*, 303 (2024) 117463, https://doi.org/10.1016/j.engstruct.2024.117463, 2024.
65. Al-Subaihawi, S., Ricles, J., Quiel, S, and T. Marullo, "Development of Multi-directional Real-Time Hybrid Simulation for Tall Buildings Subject to Multi-natural Hazards," *Engineering Structures*, 315 (2024) 118348, https://doi.org/10.1016/j.engstruct.2024.118348, 2024.
66. Al-Subaihawi, S., Ricles, J., Quiel, S., T. Marullo, and F. Malik, "Real-Time Hybrid Simulation of Structural Systems with Soil-Foundation Interaction Effects Using Neural Networks," *Earthquake Engineering and Structural Dynamics*, 53(15) 4688-4718. https://doi.org/10.1002/eqe.4236, 2024.
67. Abu-Kassab, Q., Suleiman, M., Ricles, J.M., Sause, R.; and Marullo, T. "Large-scale Multidirectional Soil-Foundation-Structure Interaction Testing of Renewable Energy Systems," *Ocean Engineering*, 323 (2025) 120595, https://doi.org/10.1016/j.oceaneng.2025.120595, 2025.
68. Malik, F. Gorini, D.N, Ricles, J., and M. Rahnesmoonfar, "Multi-Physics Framework for Seismic Real-time Hybrid Simulation of Soil-Foundation-Structural Systems," *Engineering Structures*, 334 (2025) 120247, https://doi.org/10.1016/j.engstruct.2025.120247, 2025.
69. Cao, L., Marullo, M., Ricles, J., Sause, R., Reis, C., and J. Saunders, "Recent Developments and Discoveries in Natural Hazards Mitigation Research at the NHERI Lehigh Experimental Facility," *Frontiers in Built Environment*, Volume 11 – 2025, doi: 10.3389/fbuil.2025.1567729, 2025.
70. Malik, F., Ricles, J., Cao, L., Downey, A. "Online Cyber-Physical Neural Network Model for Real-time Hybrid Simulation," *Earthquake Engineering and Structural Dynamics*, under review for publication, 2025.

7 of 7

© Ricles and Malik, 2025

Acknowledgements

- The following Lehigh University colleagues, former graduate student, and external institution contributions are gratefully acknowledged:
  - Professor Richard Sause (Joseph Stuart Professor, Lehigh University)
  - Thomas Marullo (Lehigh NHERI Research Scientist & IT Systems)
  - Dr. Liang Cao (Lehigh NHERI Research Scientist)
  - Professor Safwan Al-Subaihawi (Cal Polytechnic San Luis Obispo)
  - Faisal Malik (current Lehigh PhD student)
  - Qasim Abu-Kassab (current Lehigh PhD student)
  - Professor Cheng Chen (San Francisco State)
  - Professor Oya Mercan (University of Toronto)
  - Professor Chinmoy Kolay (India Institute of Technology Kanpur)
  - Professor Yunbyeong Chae (Seoul National University)
  - Professor Theodore Karavasilis (University of Patras)
  - Dr. Baiping Dong (Tongji University)
  - Professor Ricardo Herrera (University of Chile)
  - Dr. Davide Noè Gorini (Sapienza Univ of Rome)
  - Dr. Choung-Yeol Seo (Bechtel Corporation)
  - Dr. Ying-Cheng Lin (NCREE Taiwan)
  - Professor Maryam Rahnemoonfar (Lehigh University)
  - Professor Muhannad Suleiman (Lehigh University)
  - Professor Spencer Quiel (Lehigh University)
  - Dr. Akbar Mahvashmohammadi (OTJJ-
  - Dr. Alia Amer (Xlsvrxsr$Xsq ewixm
  - Professor David Roke (University of Akron)
  - Dr. Brent Chancellor (WJE)
  - Dr. De-Cheng Feng (Southeast University)
  - Professor Bo Fu (Chang-an University)
  - Dr. Haithan Mohamed (Marcon Forensics)
  - Professor Amal Elawady (Florida Intl University)
  - Professor Arindam Chowdhury (Florida Intl University)

Session 1: Overview and Motivation for Using Hybrid Simulation

Resilient Structural Systems

- Resilient systems often created using response modification devices
- Performance-based design procedures require experimental validation, considering effects of:
  - ➢ Large-scale
  - ➢ Load-rate dependency
  - ➢ Realistic loading
  - ➢ Multi-directional system response
  - ➢ Interaction effects among components of the system

Assessment of large-scale systems subjected to multi-directional, multi-hazard demand in real-time

Elastomeric dampers (Kontopanos 2006)

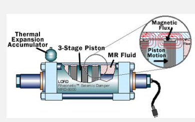

Magneto-Rheological damper (G. Yang, 2001)

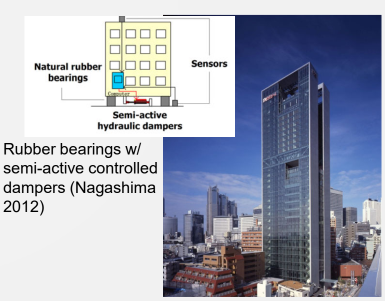

Rubber bearings w/ semi-active controlled dampers (Nagashima 2012)

Nonlinear Viscous Fluid dampers (Kolay 2016)

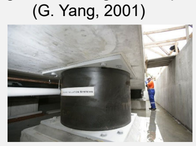

Lead-rubber bearings (CivilDigital, 2016)

What is (RT)HS? Why is it important?

(Real-Time) Hybrid Simulation

Performed in real time — Simulation of response

Cyber (analytical/numerical)
+
Physical (experimental)

- Well understood structural components
- Modelled numerically
- Various substructures possible for a given experimental substructure

- Not well understood structural components
- Modelled physically with appropriate boundary conditions
- Easy to accommodate full-scale components

- Cost effective large-scale testing method
- Integrates benefits of numerical simulations & physical tests: Best of both worlds
- Comprehensive system and component response
- Rate dependent devices can be tested

Real-time Hybrid Simulation (RTHS) Concept: Structural System Subject to Multi-Natural Hazards

Structural System

40-Story Building with Outriggers and Supplemental Dampers

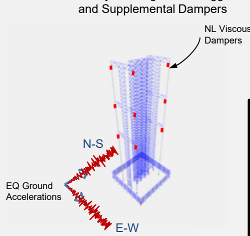

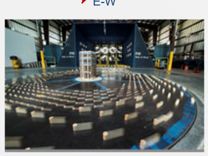

Wind Tunnel Tests NHERI@FIU
Wind Load Determination

Hybrid Earthquake Simulation Experiments

Real-time input EQ ground acceleration

$\mathbf{F}^a_{i+1}$ *Excitation*

Analytical substructure

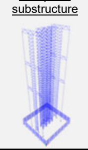

(Modeled in the computer)

Cmd Displ $\mathbf{X}^a_{i+1}$

$\mathbf{R}^a_{i+1}$ *Restoring Force*

Simulation Coordinator

$$\mathbf{M}\ddot{\mathbf{X}}_{i+1} + \mathbf{C}\dot{\mathbf{X}}_{i+1} + \mathbf{R}^a_{i+1} + \mathbf{R}^e_{i+1} = \mathbf{F}^a_{i+1}$$

Integrates Eqns of Motion

Cmd Displ $\mathbf{X}^e_{i+1}$

$\mathbf{R}^e_{i+1}$ *Restoring Force*

Experimental substructure (dampers)

(Modeled in lab)

Real-time structural response

If the real-time hybrid simulation processes do not remain synchronization within the time step Δt. This leads to an inaccurate result and potential instability.
Digital Controllers: 1024 to 2048 Hz -> Δt ∝ 1/2048 to 1/1024 sec

Selected RTHS Examples

Steel Structure with Nonlinear Viscous Dampers Studied using Large-scale RTHS

- **Prototype building**
  - 3-story, 6-bay by 6-bay office building located in Southern California
  - Moment resisting frame (MRF) with RBS beam-to-column connections, damped brace frame (DBF), gravity load system, inherent damping of building

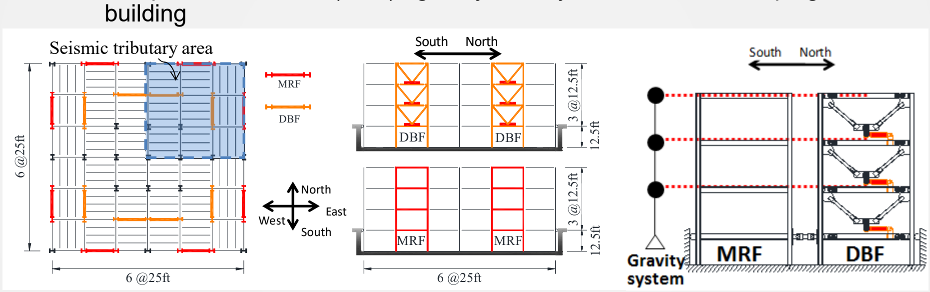

Plan view of prototype building **Section view of prototype building** **Test structure**

Dong, B., Sause, R., and J.M. Ricles, (2015) "Accurate Real-time Hybrid Earthquake Simulations on Large-scale MDOF Steel Structure with Nonlinear Viscous Dampers," Earthquake Engineering and Structural Dynamics, 44(12) 2035–2055, https://DOI.org/10.1002/eqe.2572.
Dong, B., Sause, R., and J.M. Ricles, (2016) "Seismic Response and Performance of Steel MRF Building with Nonlinear Viscous Dampers under DBE and MCE," Journal of Structural Engineering, 142(6) https://DOI.org/10.1061/(ASCE)ST.1943-541X.0001482.

Nonlinear Viscous Dampers

Characterization testing

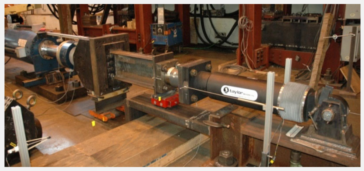

Damper testbed

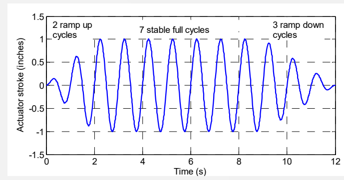

Loading Protocol

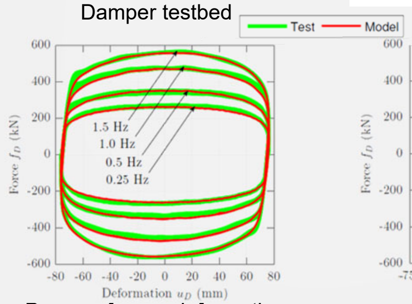

Damper force - deformation

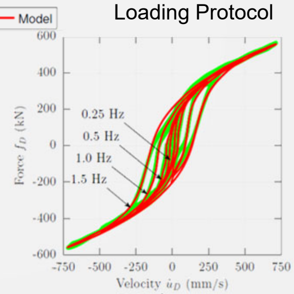

Damper force - velocity

LEHIGH UNIVERSITY | ATLSS | RTMD | NSF 75 YEARS OF DISCOVERY & INNOVATION | NSF NHERI CYBER-PHYSICAL SIMULATION

Large-scale RTHS on Structure with Nonlinear Viscous Dampers: Substructures

Substructures for RTHS Phase-1

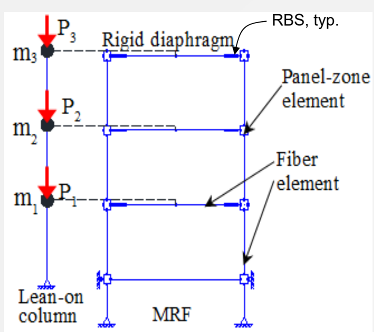

Analytical substructure (MRF, mass, gravity system, inherent damping)

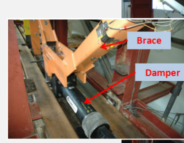

Experimental substructure (0.6-scale DBF)

Real-time state determination

- Analytical substructure has 296 DOFs and 91 elements;
- Nonlinear fiber elements for beams, columns, and RBS;
- Nonlinear panel zone elements for panel zone of beam-column connection;
- Elastic beam-column element for the lean-on column;
- P-delta effects included in the analytical substructure.
- Δt = 3/1024 sec.

Phase 1 Large-Scale Real-Time Hybrid Simulation

(MRF, Floor Diaphragm, Gravity System, Mass, Inherent Mass in Analytical Substructure)

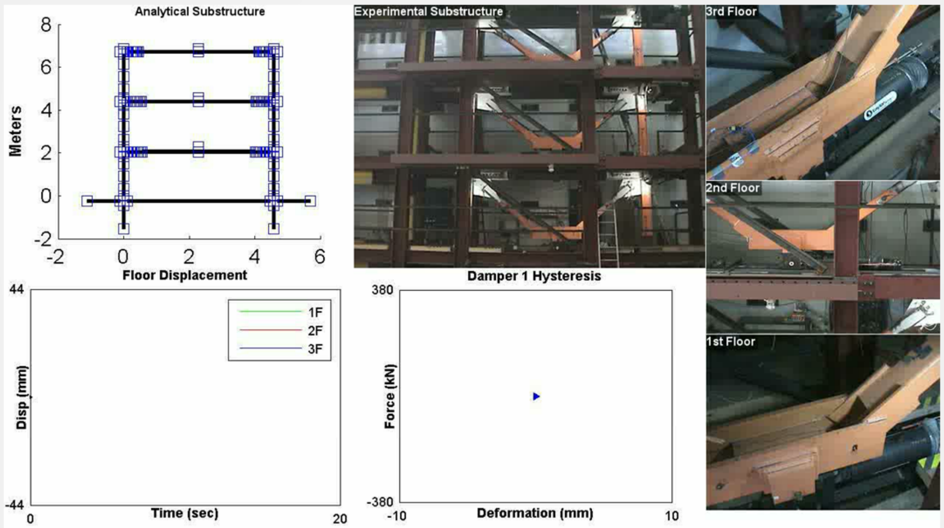

17

Phase 2 Real-Time Hybrid Simulations on MRF Building Structure with Nonlinear Viscous Dampers (MCE)

Comparison of Phase-1 and Phase-2 RTHS Results (Validate Phase-1 Analytical Substructure)

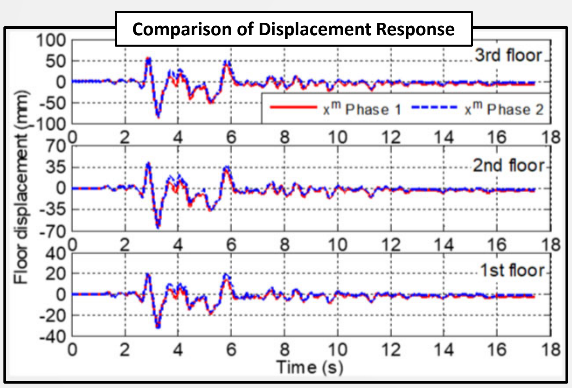

Maximum peak displacement difference: 2.1, 1.7, 1.8 mm (6.8%, 2.7%, 2.1%)

Phase-1

Phase-2

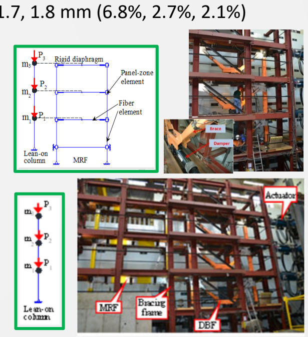

1994 Northridge Earthquake record RRS318 component scaled to MCE (~2500yr)

Dong, B., Sause, R., and J.M. Ricles, (2015) "Accurate Real-time Hybrid Earthquake Simulations on Large-scale MDOF Steel Structure with Nonlinear Viscous Dampers," Earthquake Engineering and Structural Dynamics, 44(12) 2035–2055, https://DOI.org/10.1002/eqe.2572.

18

Phase-1 Real-Time Hybrid Simulations on MRF Building Structure with Nonlinear Viscous Dampers

Phase-1 Real Time Hybrid Simulations (RTHS)

- Experimental substructure (DBF with dampers) is undamaged by DBE and MCE input; damage is confined to MRF within analytical substructure; enable use of new, undamaged MRF for each simulation
- Therefore, an ensemble of ground motion records could be used in Phase-1 RTHS to account for record-to-record variability

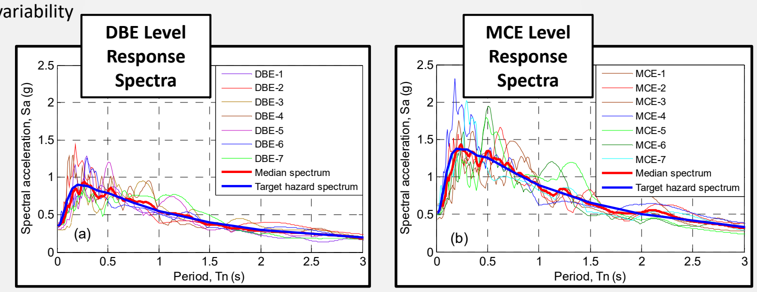

Dong, B., Sause, R., and J.M. Ricles, "Seismic Response and Performance of Steel MRF Building with Nonlinear Viscous Dampers under DBE and MCE," Journal of Structural Engineering, 142(6) https://DOI.org/10.1061/(ASCE)ST.1943-541X.0001482, 2016.

Response of RTHS Phase-1

- Response structure to Design Basis Earthquake (DBE) and Maximum Considered Earthquake (MCE) level RTHS
- Structure designed for 100% (D100V), 75% (D75), and 60% of the Design Base Shear.

Peak story drift ratios

Structure	DBE			MCE		
	Mean (% rad)			Mean (% rad)		
	1st story	2nd story	3rd story	1st story	2nd story	3rd story
D100V	0.69	0.76	0.53	1.20	1.38	1.00
D75V	0.85	0.98	0.74	1.53	1.86	1.52
D60V	1.00	1.17	0.95	1.88	2.21	1.88

Response of RTHS Phase-1

- Response structure to Design Basis Earthquake (DBE) and Maximum Considered Earthquake (MCE) level RTHS
- Structure designed for 100% (D100V), 75% (D75), and 60% of the Design Base Shear.

Residual story drift ratios

Structure	DBE			MCE		
	Mean (% rad)			Mean (% rad)		
	1st story	2nd story	3rd story	1st story	2nd story	3rd story
D100V	0.02	0.03	0.01	0.06	0.06	0.06
D75V	0.04	0.05	0.03	0.13	0.17	0.15
D60V	0.05	0.06	0.05	0.20	0.20	0.20

Phase-1 RTHS Results Evaluation

- Damper-brace interaction

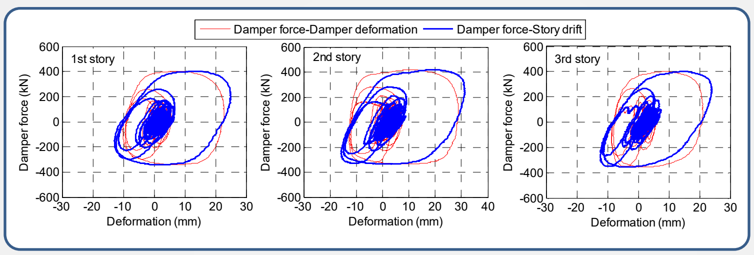

D75V structure, DBE level RTHS, PTS315 record

- Story drifts are larger than damper deformations, which indicates elastic flexibility exists within the damper force path;
- Damper forces are larger at the times of peak story drift, which indicates the partially in-phase behavior of damper force with story drift

Dong, B., Sause, R., and J.M. Ricles, "Seismic Response and Performance of Steel MRF Building with Nonlinear Viscous Dampers under DBE and MCE," Journal of Structural Engineering, 142(6) https://DOI.org/10.1061/(ASCE)ST.1943-541X.0001482, 2016.

Phase-1 Real-Time Hybrid Simulations of MRF Building Structure with Nonlinear Viscous Dampers

Seismic Fragility Curve: Probabilistic Assessment of a Structure's Performance in terms of a Engineering Demand Parameter (e.g., Peak Story Drift)

Experimental substructure (DBF with dampers) is undamaged; enables use of undamaged MRF in analytical substructure for each simulation; an ensemble of ground motion records was used to account for record-to-record variability

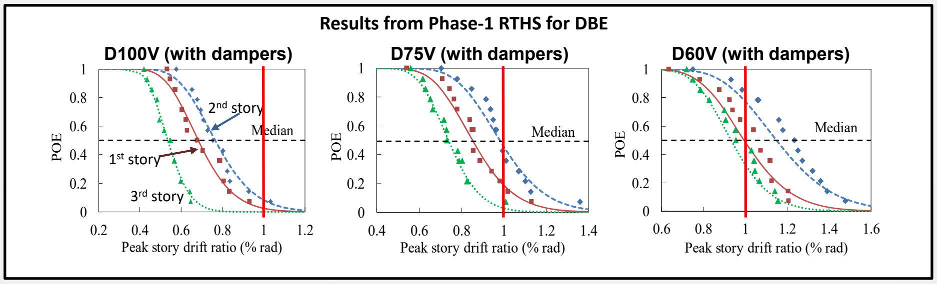

Dong, B., Sause, R., and J.M. Ricles, "Seismic Response and Performance of Steel MRF Building with Nonlinear Viscous Dampers under DBE and MCE," Journal of Structural Engineering, 142(6) https://DOI.org/10.1061/(ASCE)ST.1943-541X.0001482, 2016.

Damped Systems Summary

Damped systems… reducing lateral drift without increasing accelerations

- Steel building structures (e.g., MRFs) with dampers can have significantly enhanced performance relative to conventional steel MRFs
- Elastic flexibility in the damper force path causes the viscous damper forces to be partially in phase with the story drift resulting in combined column response with large axial force at the time of peak bending moment. These combined column demands should be considered in the design of frames with nonlinear viscous dampers
- D75 and D60V MRFs with dampers (75% and 60% Design Base Shear):
  - Demonstrated that reduced-strength MRFs with dampers perform well compared to conventional MRFs
  - Performance is between "Immediate Occupancy" and "Life Safety" for DBE and MCE
  - Significantly better performance than conventional steel MRF

Tall Building Subject to Multi-natural Hazards

- 40-story (+4 basement) BRBF building in Los Angeles designed by SGH[1] for PEER Tall Building Initiative case studies – BRBFs with Outriggers
- Objectives of study
  - Improve performance using nonlinear fluid viscous dampers with outriggers
  - Assess performance of structure under multi-hazards using RTHS.

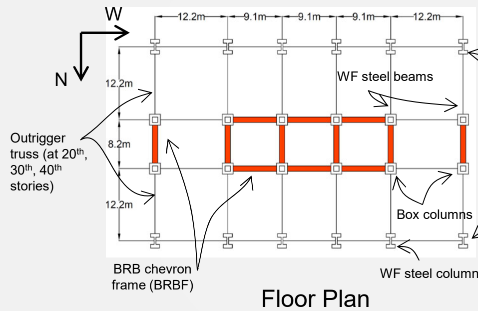

Floor Plan

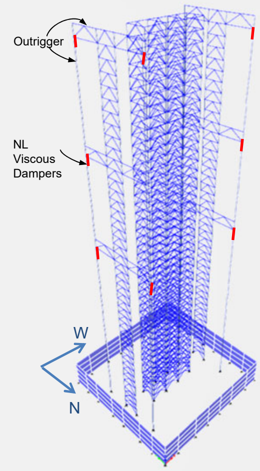

[1] Moehle et al., PEER 2011/05

Al-Subaihawi, S., Kolay, C., Thomas Marullo, Ricles, J. M. and S. E. Quiel, "Assessment of Wind-Induced Vibration Mitigation in a Tall Building with Damped Outriggers Using Real-time Hybrid Simulations," *Engineering Structures*, 205, https://doi.org/10.1016/j.engstruct.2019.110044, 2020.

Kolay, C., Al-Subaihawi, S., Thomas Marullo, Ricles, J. M. and S. E. Quiel, "Multi-Hazard Real-Time Hybrid Simulation of a Tall Building with Damped Outriggers," *International Journal of Lifecycle Performance Engineering*, Vol. 4, Nos. 1/2/3, pp.103–132, https://doi.org/10.1504/IJLCPE.2020.10893, 2020.

Multi-Hazard 3-D Nonlinear RTHS of Tall Building – EQ & Wind

- Bidirectional EQ ground motions
  - ➢ 1989 Loma Prieta EQ – Saratoga Aloha Ave Station scaled to MCE (2500 year return period) hazard level
- Bidirectional wind loading
  - ➢ Wind speed of 110 mph, 700 MRI
  - ➢ Exposure B

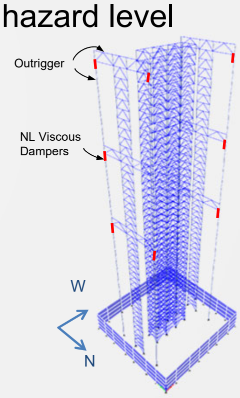

RTHS Substructures

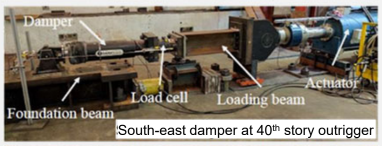

Experimental Substructure –
NL Fluid Viscous Damper

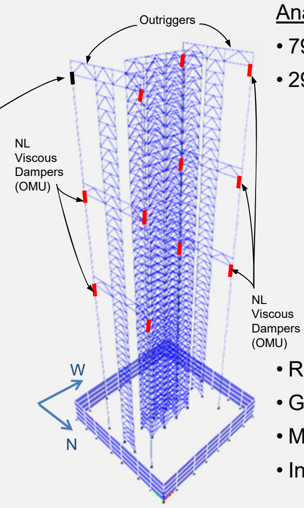

Analytical Substructure

<u>Analytical Sub. Key features</u>:

- 7902 DOF
- 2974 Elements
  - 2411 Nonlinear Explicit Force-based fiber elements
  - 11 Nonlinear Explicit Maxwell Elements(1) with real-time on-line model updating (dampers placed in each outrigger at 20th, 30th, & 40th floors)
  - 552 Nonlinear truss elements to model Buckling Restrained Braces (BRBs)
- Reduced Order Modeling
- Geometric nonlinearities
- Mass
- Inherent damping of building

(1) Al-Subaihawi, S. (2023). *Real-time Hybrid Simulation of Complex Structural Systems Subject to Multi-Hazards.* PhD Dissertation, CEE Dept., Lehigh University.

3-D Real-time Hybrid Simulation
1989 Loma Prieta EQ Bidirectional Ground Motions Scaled to MCE

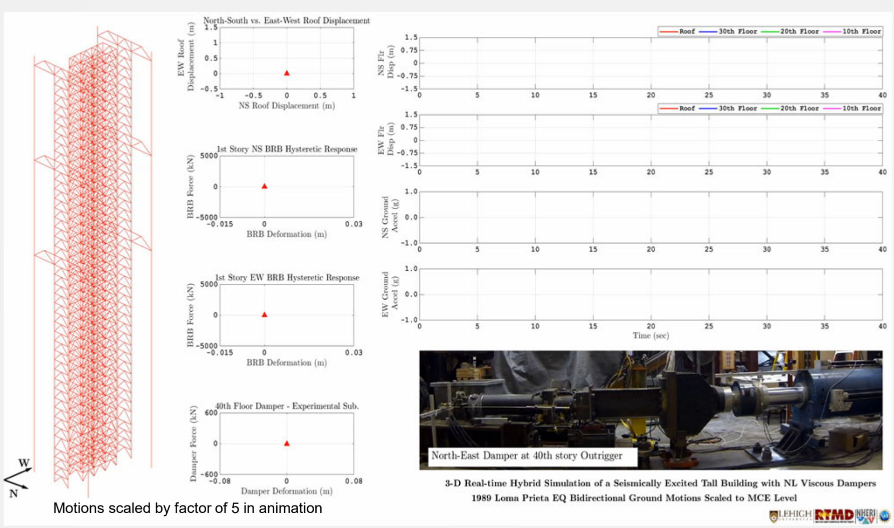

Al-Subaihawi, S., Ricles, J., Quiel, S, and T. Marullo, "Development of Multi-directional Real-Time Hybrid Simulation for Tall Buildings Subject to Multi-natural Hazards," *Engineering Structures*, 315 (2024) 118348, https://doi.org/10.1016/j.engstruct.2024.118348, 2024.

3-D Real-time Hybrid Simulation
110 mph, 700 MRI Wind Storm (EW Windward Direction)

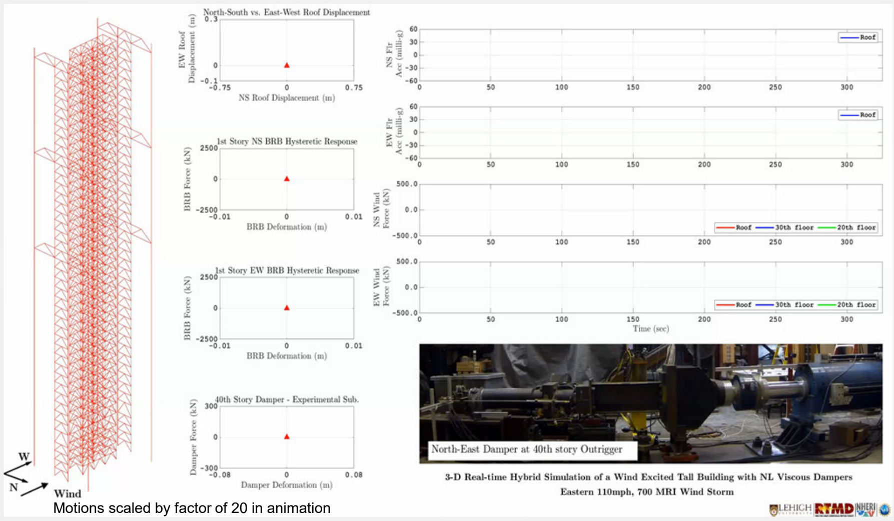

Al-Subaihawi, S., Ricles, J., Quiel, S, and T. Marullo, "Development of Multi-directional Real-Time Hybrid Simulation for Tall Buildings Subject to Multi-natural Hazards," *Engineering Structures*, 315 (2024) 118348, https://doi.org/10.1016/j.engstruct.2024.118348, 2024.

3-D RTHS Results: Roof Lateral Accelerations
Wind from East @ 110 mph, 700 Year MRI

Floor Accelerations - NS direction

Peak Floor Accelerations

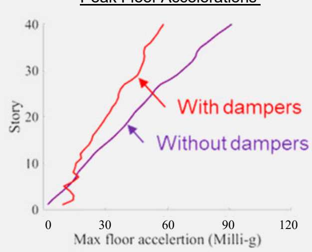

RMS Floor Accelerations

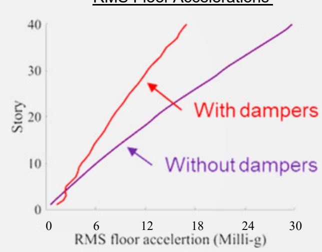

- Peak Acceleration: 35% reduction in NS,10% reduction in EW
- RMS Acceleration: 49% reduction in NS, 2% reduction in EW

Note: Outrigger frames are in NS direction

3-D RTHS Results: Story Drift
1989 Loma Prieta EQ Scaled to MCE

Story Drift- NS direction

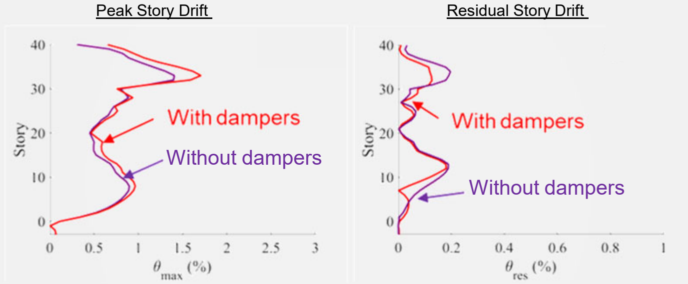

- Peak Story Drift: 20% increase in NS, Minimal change in EW
- Residual Story Drift: 48% reduction in NS, Minimal reduction in EW
- BRB ductility demand: Minimal reduction in EW, 30% reduction in NS

Note: Outrigger frames are in NS direction

© Ricles and Malik, 2025

3-D RTHS Results: Story Drift
1989 Loma Prieta EQ Scaled to MCE

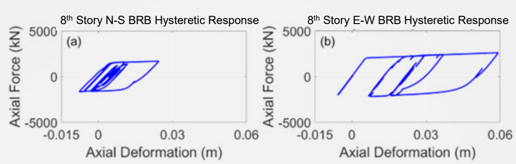

BRB force-deformation response under earthquake RTHS in (a) N-S and (b) E-W directions in BRBFs 1 and 3

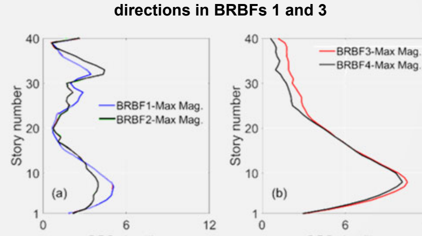

Peak magnitude of BRBF ductility over the height of the building in the (a) N-S and (b) E-W directions of selected BRBFs 1, 2, 3, and 4

Al-Subaihawi, S., Ricles, J., Quiel, S, and T. Marullo, "Development of Multi-directional Real-Time Hybrid Simulation for Tall Buildings Subject to Multi-natural Hazards," *Engineering Structures*, 315 (2024) 118348, https://doi.org/10.1016/j.engstruct.2024.118348, 2024.

Member Stiffness in Damper Force Load Path – 700 Year MRI Wind

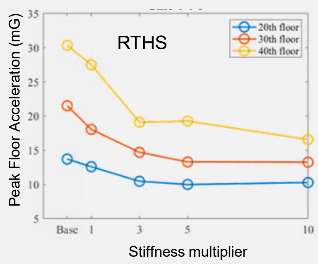

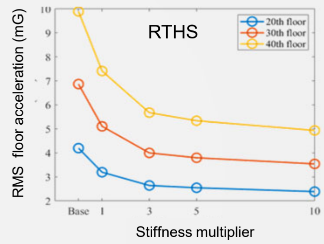

- Outrigger truss members' and columns' axial stiffness increased using stiffness multiplier in analytical substructure
- A larger member's stiffness results in an increase in the deformations being concentrated in the dampers
- Inefficient to increase stiffness multiplier beyond value of 3.0

Al-Subaihawi, S., Kolay, C., Thomas Marullo, Ricles, J. M. and S. E. Quiel, "Assessment of Wind-Induced Vibration Mitigation in a Tall Building with Damped Outriggers Using Real-time Hybrid Simulations," *Engineering Structures*, 205, https://doi.org/10.1016/j.engstruct.2019.110044, 2020.

33

JR [2]3

Session 2: Hybrid Simulation Background and Theory

34

RTHS: Implementation issues and challenges

Simulation coordinator

- Numerical integration algorithm
  - Accurate
  - Explicit
  - Unconditionally stable
  - Dissipative

  Preferred
- Fast communication

Analytical substructure

- Fast and accurate state determination procedure for complex structures

Experimental substructure

- Large capacity hydraulic system and dynamic actuators required
- Actuator kinematic compensation
- Robust control of dynamic actuators for large-scale structures

Direct Integration Algorithms

Background – Numerical Direct Integration Algorithms

Direct Integration Algorithms

Implicit
- Iterative
- Can provide unconditional stability
- Convergence problems!

Explicit
- Noniterative
- Conditionally stable
- Sometimes preferred for highly nonlinear problems

Conditionally stable
$\Delta t \propto \frac{1}{\omega_{max}}$

Unconditionally stable
Δt governed by accuracy

Nondissipative

Dissipative

Model-based algorithms

Dahlquist theorem (1963): explicit algorithms cannot be unconditionally stable

Preferred for numerical simulation
- ✓ Unconditionally stable → implicit
- ✓ Second-order accurate
- ✓ Parametrically dissipative
- ✓ Example: HHT-α, WBZ-α, G-α

Preferred for seismic HS and RTHS
- ✓ Explicit
- ✓ Second-order accurate
- ✓ Unconditionally stable
- ✓ Parametrically dissipative
- ✓ Example: limited study

HS: Hybrid simulation; RTHS: Real-time hybrid simulation

Integration Algorithm

- Integration Algorithm Desirable (required) characteristics

  - Explicit formulation
  - Unconditional stability
  - Controllable numerical damping
  - Improved overshoot for high-frequency modes
  - Improved stability for nonlinear stiffening type systems

Modified KR-α (MKR- α) method

Kolay, C., & Ricles, J. M. (2014). Development of a family of unconditionally stable explicit direct integration algorithms with controllable numerical energy dissipation. *Earthquake Engineering and Structural Dynamics*, *43*(9), 1361–1380. http://doi.org/10.1002/eqe.2401

RTHS: Essentials of Discrete Control Theory [Ogata 1995]

- Temporally discretized form of equations of motion

$$m \cdot \ddot{x}_{i+1} + 2m\xi\omega_n \cdot \dot{x}_{i+1} + m\omega_n^2 \cdot x_{i+1} = F_{i+1}$$

- Z-transform for a discrete system

$$Z\{F(k)\} = F(z) = \sum_{k=0}^{\infty} F(k) \cdot z^{-k}$$

- The real translation theorem

$$Z\{F(k-1)\} = z^{-1} \cdot F(z)$$

- Discrete transfer function G(z)

$$G(z) = \frac{X(z)}{F(z)} = \frac{n_r z^r + \cdots + n_1 z + n_0}{d_q z^q + \cdots + d_1 z + d_0}$$

X(z) = input
F(z) = output

E.g., for Equations of motion $G(z) = \frac{x(z)}{F(z)} = \frac{\Delta t^2 \cdot z^2 + 2 \cdot \Delta t^2 \cdot z + \Delta t^2}{\left[(4 + \omega_n{}^2 \Delta t^2 + 4\xi\omega_n \Delta t)z^2 + (-8 + 2\omega_n{}^2 \Delta t^2)z + (4 - 4\xi\omega_n \Delta t + \omega_n{}^2 \Delta t^2)\right]m}$

Ogata, K. (1995). *Discrete-Time Control Systems* (2nd ed.). Englewood Cliffs, NJ: Prentice Hall

RTHS: Essentials of Discrete Control Theory

- Block diagrams

open loop

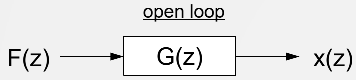

$$G(z) = \frac{x(z)}{F(z)}$$

closed loop

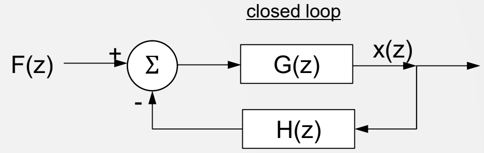

$$B(z) = \frac{x(z)}{F(z)} = \frac{G(z)}{1 + G(z)H(z)}$$

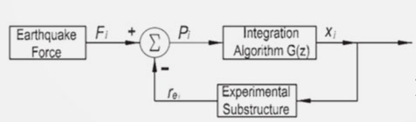

x_i : Displacement vector
r_e : Restoring force vector

Block diagram representation of real-time hybrid simulation

RTHS: Essentials of Discrete Control Theory

- Root locus: closed-loop system

$$\mathrm{B}(z) = \frac{x(z)}{F(z)} = \frac{G(z)}{1 + G(z)H(z)}$$

- Roots of numerator of G(z) are *open zeros*
- Roots of denominator of G(z) are *open poles*
- Roots of numerator of B(z) are *closed-loop zeros*
- Roots of denominator of B(z) are *closed-loop poles*

Unit Circle in complex plane:

- Closed-loop poles migrate from open-loop poles to open-loop zeros
- If closed-loop poles stay on, or within the unit circle then closed-loop system is stable

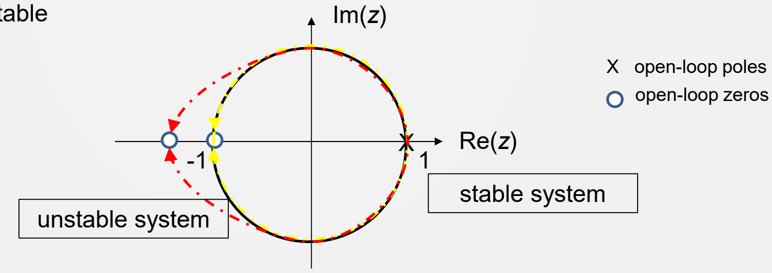

Analysis of an Integration Algorithm

- Discrete transfer function of an integration algorithm in z-domain

$$G(z) = \frac{X(z)}{F(z)} = \frac{n_3 z^3 + n_2 z^2 + n_1 z + n_0}{d_3 z^3 + d_2 z^2 + d_1 z + d_0}$$

Roots of numerator polynomial = zeros

Roots of denominator polynomial = poles

$n_0 \ldots n_3$: numerator coefficients
$d_0 \ldots d_3$: denominator coefficients
$X(z)$: z-transform of x_{n+1}
$F(z)$: z-transform of f_{n+1}

$X(z)$: output
$F(z)$: input

- $G(z)$ is a function of m, $\Omega = \omega\Delta t$, ξ, and algorithmic parameters

- Poles govern numerical dispersion (period error) and dissipation (equivalent damping ratio), and stability characteristics

- Want algorithm to be second-order and not too dissipative for important low-frequency modes

Implicit G-α Method (Chung & Hulbert, 1993)

- Weighted equation of motion; concept introduced by Hilber et al., 1977

$$m[(1-\alpha_m)\ddot{x}_{n+1}+\alpha_m\ddot{x}_n]+c[(1-\alpha_f)\dot{x}_{n+1}+\alpha_f\dot{x}_n]+k[(1-\alpha_f)x_{n+1}+\alpha_f x_n] = (1-\alpha_f)f_{n+1}+\alpha_f f_n$$

- At $t_n = 0$ $\quad m\ddot{x}_0 + c\dot{x}_0 + kx_0 = f_0$
- Adopts displacement and velocity difference equations of Newmark method
- α_m, α_f, γ, & β are related to $\rho_\infty \in [1,0]$ to achieve unconditional stability, second-order accuracy, and an optimal dissipation characteristic

Proposed Explicit KR-α & MKR-α Method: SDOF Systems

- Difference equations

Displacement (explicit): $x_{n+1} = x_n + \Delta t\dot{x}_n + \Delta t^2\alpha_2\ddot{x}_n$

Velocity (explicit): $\dot{x}_{n+1} = \dot{x}_n + \Delta t\alpha_1\ddot{x}_n$

- How to develop an explicit (E) method which will inherit 3 poles of G-α method?
- Need 3 model-based parameters (α_1, α_2, and α_3)
- Modify weighted equation of motion of G-α method by introducing α_3

$$m[(1-\alpha_3)\ddot{x}_{n+1}+\alpha_3\ddot{x}_n]+c[(1-\alpha_f)\dot{x}_{n+1}+\alpha_f\dot{x}_n]+k[(1-\alpha_f)x_{n+1}+\alpha_f x_n] = (1-\alpha_f)f_{n+1}+\alpha_f f_n$$

Proposed Explicit-α method: SDOF systems

- Determine α_1, α_2, and α_3 so that E-α method inherits 3 poles of G-α method

$$G(z) = \frac{X(z)}{F(z)} = \frac{n_3 z^3 + n_2 z^2 + n_1 z + n_0}{d_3 z^3 + d_2 z^2 + d_1 z + d_0}$$

Characteristic equations:

G-α method: $d_3^{\alpha} z^3 + d_2^{\alpha} z^2 + d_1^{\alpha} z + d_0^{\alpha} = 0$

E-α method: $d_3^{New} z^3 + d_2^{New} z^2 + d_1^{New} z + d_0^{New} = 0$

Make identical

$$\alpha_1 = \frac{(1+2\gamma\xi\Omega)}{1+2\gamma\xi\Omega+\beta\Omega^2}; \qquad \alpha_2 = \frac{1}{2}\frac{[1+2(\gamma-2\beta)\xi\Omega]}{[1+2\gamma\xi\Omega+\beta\Omega^2]}; \qquad \alpha_3 = \frac{\alpha_m+2\alpha_m\gamma\xi\Omega+\alpha_f\beta\Omega^2}{1+2\gamma\xi\Omega+\beta\Omega^2}$$

- α_1, α_2, and α_3 are functions of model parameters ξ, Ω, and integration parameters α_m, α_f, γ, and β, as intended

Proposed Explicit-α method: MDOF systems

Displacement (explicit): $\mathbf{X}_{n+1} = \mathbf{X}_n + \Delta t \dot{\mathbf{X}}_n + \Delta t^2 \boldsymbol{\alpha}_2 \ddot{\mathbf{X}}_n$

Velocity (explicit): $\dot{\mathbf{X}}_{n+1} = \dot{\mathbf{X}}_n + \Delta t \boldsymbol{\alpha}_1 \ddot{\mathbf{X}}_n$

$$\mathbf{M}[(\mathbf{I}-\boldsymbol{\alpha}_3)\ddot{\mathbf{X}}_{n+1} + \boldsymbol{\alpha}_3\ddot{\mathbf{X}}_n] + \mathbf{C}[(1-\alpha_f)\dot{\mathbf{X}}_{n+1} + \alpha_f\dot{\mathbf{X}}_n] + \mathbf{K}[(1-\alpha_f)\mathbf{X}_{n+1} + \alpha_f\mathbf{X}_n] = (1-\alpha_f)\mathbf{F}_{n+1} + \alpha_f\mathbf{F}_n$$

- Model-based parameters:

$$\boldsymbol{\alpha}_1 = \boldsymbol{\alpha}^{-1}\mathbf{M}$$

$$\boldsymbol{\alpha}_2 = \left(\frac{1}{2}+\gamma\right)\boldsymbol{\alpha}_1$$

$$\boldsymbol{\alpha}_3 = \boldsymbol{\alpha}^{-1}[\alpha_m\mathbf{M} + \alpha_f\gamma\Delta t\mathbf{C} + \alpha_f\beta\Delta t^2\mathbf{K}]$$

where $\boldsymbol{\alpha} = [\mathbf{M} + \gamma\Delta t\mathbf{C} + \beta\Delta t^2\mathbf{K}]$

- $\boldsymbol{\alpha}_1$ and $\boldsymbol{\alpha}_2$ are related by a scalar

Model-based Integration Parameters

- $\boldsymbol{\alpha_1}$, $\boldsymbol{\alpha_2}$, and $\boldsymbol{\alpha_3}$ are functions of system matrices $\mathbf{M}$, $\mathbf{C}$, and $\mathbf{K}$
- For RTHS, $\boldsymbol{\alpha_1}$, $\boldsymbol{\alpha_2}$, and $\boldsymbol{\alpha_3}$ need to include experimental substructure matrices
- For RTHS use
  - $\mathbf{M}_{IP} = \mathbf{M} + \mathbf{M}^e$
    - $\mathbf{M}$: analytically defined mass matrix that exclude $\mathbf{M}^e$
    - $\mathbf{M}^e$: mass matrix for experimental substructure
  - $\mathbf{C}_{IP} = \mathbf{C} + \mathbf{C}_{eq}^a + \mathbf{C}_{eq}^e$
    - $\mathbf{C}$: analytically defined inherent damping matrix
    - $\mathbf{C}_{eq}^a$ and $\mathbf{C}_{eq}^e$: equivalent damping matrices associated with supplemental damping devices, if any, in analytical and experimental substructures, respectively
  - $\mathbf{K}_{IP} = \mathbf{K}_I^a + \mathbf{K}_{eq}^e$
    - $\mathbf{K}_I^a$: initial elastic stiffness matrix of analytical substructure
    - $\mathbf{K}_{eq}^e$: equivalent initial elastic stiffness matrix of experimental substructure

MKR-α Method: Dissipative Characteristics

- One parameter (ρ_∞) family of algorithms
  - ➢ ρ_∞ = spectral radius when $\Omega = \omega_n \Delta t \to \infty$
    - ✓ varies in the range $0 \le \rho_\infty \le 1$
- ρ_∞ controls numerical energy dissipation
  - ➢ $\rho_\infty = 1$: No numerical energy dissipation
  - ➢ $\rho_\infty = 0$: Asymptotic annihilation

$$\alpha_f = \frac{\rho_\infty}{\rho_\infty + 1}, \qquad \alpha_m = \frac{2\rho_\infty{}^3 + \rho_\infty{}^2 - 1}{\rho_\infty{}^3 + \rho_\infty{}^2 + \rho_\infty + 1}, \qquad \gamma = \frac{1}{2} - \alpha_m + \alpha_f, \qquad \beta = \frac{1}{2}\left(\gamma + \frac{1}{2}\right)$$

$\bar{\Omega} = \bar{\omega}\Delta t$, Normalized apparent frequency

$\bar{\xi}$ = Equivalent damping ratio

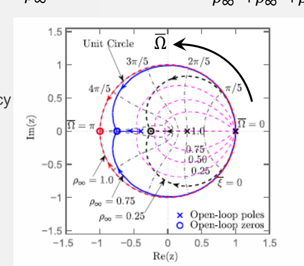

Stability: Root-Loci

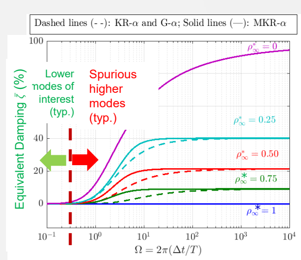

Controlled Numerical Damping

Kolay, C., and J.M. Ricles, (2017) "Improved Explicit Integration Algorithms for Structural Dynamic Analysis with Unconditional Stability and Controllable Numerical Dissipation," *Journal of Earthquake Engineering*, DOI: 10.1080/13632469.2017.1326423.

Demonstration of Numerical Dissipation

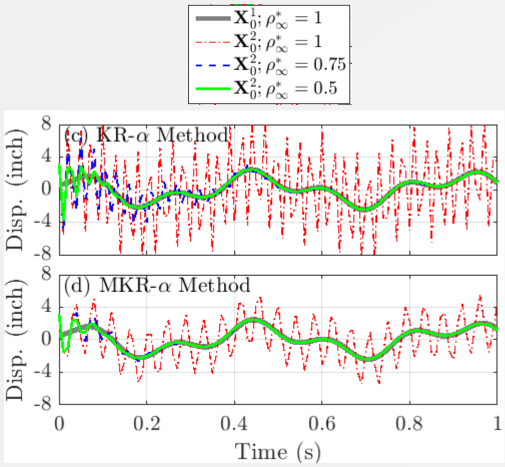

- 3-DOF system with a very high-frequency for third mode

$$\omega_1 = 13.72,\ \omega_2 = 36.08, \text{ and } \omega_3 = 504.99 \text{ rad/s}$$

$$\phi_1 = [\ 0.9506 \quad 1.5433 \quad 1.5445\ ]^T$$
$$\phi_2 = [\ 1.5587 \quad -0.9412 \quad -0.9461\ ]^T$$
$$\phi_3 = [\ 0.0005 \quad -0.2561 \quad 12.7823\ ]^T$$

- Response for zero initial velocity and initial displacements:

$$\mathbf{X}_0^1 = (\phi_1 + \phi_2) \text{ inches and } \mathbf{X}_0^2 = (\phi_1 + \phi_2 + 0.2\phi_3)$$

- Low-frequency mode response is negligibly influenced by numerical dissipation
- MKR-α possess better dissipative characteristics

MCE* level RTHS using $\rho_\infty = 1.0$

* Maximum considered EQ, return period = 2474 years

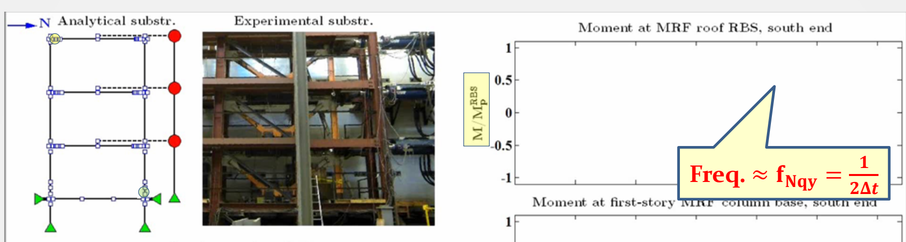

- Under nonlinear structural behavior, pulses are introduced in the acceleration at the Nyquist frequency $\left(= \frac{1}{2\Delta t}\right)$ when the state of the structure changes within the time step
- Pulses excite spurious higher modes present in the system which primarily contribute to the member forces
- Problem becomes worst by the noise introduced through the measured restoring forces and the actuator delay compensation which can amplify high frequency noise.

Kolay, C., Ricles, J., Marullo, T., Mahvashmohammadi, A., and Sause, R. (2015). Implementation and application of the unconditionally stable explicit parametrically dissipative KR-α method for real-time hybrid simulation. *Earthquake Engineering & Structural Dynamics*. 44, 735-755, doi:10.1002/eqe.2484.

MCE level RTHS using $\rho_\infty = 0.75$

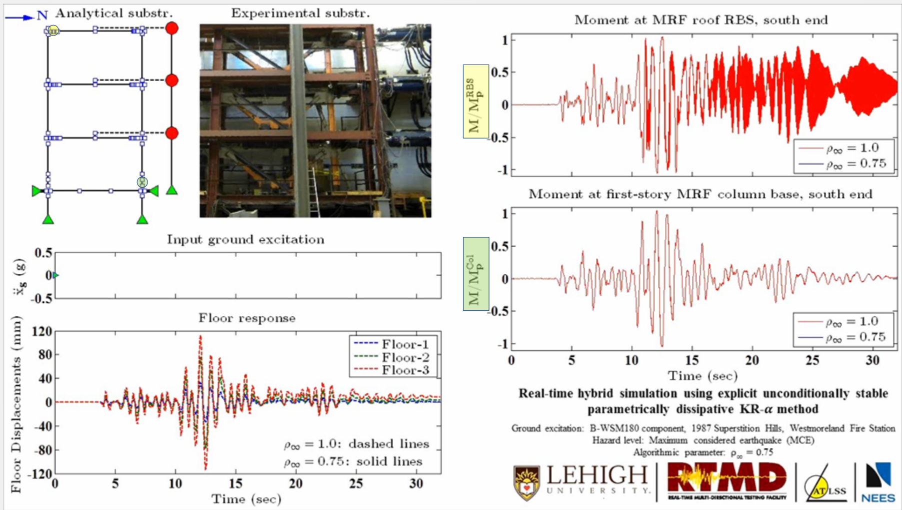

Kolay, C., Ricles, J., Marullo, T., Mahvashmohammadi, A., and Sause, R. (2015). Implementation and application of the unconditionally stable explicit parametrically dissipative KR-α method for real-time hybrid simulation. *Earthquake Engineering & Structural Dynamics*. 44, 735-755, doi:10.1002/eqe.2484.

Numerical Stability: Nonlinear SDOF Systems

- Employ the concept of linearized stability
  - Provides necessary stability conditions which may not be sufficient
- Consider a linear SDOF system first

$$m\hat{\ddot{x}}_{n+1} + c\dot{x}_{n+1-\alpha_f} = f_{n+1-\alpha_f} - kx_{n+1-\alpha_f} \stackrel{\text{def}}{=} l_{n+1}$$

Where

$$\hat{\ddot{x}}_{n+1} = (1-\alpha_3)\ddot{x}_{n+1} + \alpha_3\ddot{x}_n$$

$$(\cdot)_{n+1-\alpha_f} = (1-\alpha_f)(\cdot)_{n+1} + \alpha_f(\cdot)_n$$

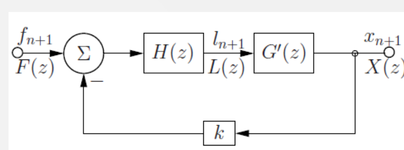

$$H(z) = \frac{L(z)}{F(z) - kX(z)} = (1-\alpha_f) + \frac{\alpha_f}{z}$$

$$G'(z) = \frac{n_3'z^3 + n_2'z^2 + n_1'z + n_0'}{d_3'z^3 + d_2'z^2 + d_1'z + d_0'}$$

$$G_{CL}(z) = \frac{X(z)}{F(z)} = \frac{H(z)G'(z)}{1 + kH(z)G'(z)}$$

$G'(z)$ is a function of α_1, α_2, & α_3

Kolay, C., and J.M. Ricles, "Improved Explicit Integration Algorithms for Structural Dynamic Analysis with Unconditional Stability and Controllable Numerical Dissipation," *Journal of Earthquake Engineering*, 23(5), pp 771-792, http://dx.doi.org/10.1080/13632469.2017.1326423, 2019.

Numerical Stability: Nonlinear SDOF Systems

- Equation of motion for nonlinear SDOF system:

$$m\hat{\ddot{x}}_{n+1} + c\dot{x}_{n+1-\alpha_f} = f_{n+1-\alpha_f} - r_{n+1-\alpha_f} \stackrel{\text{def}}{=} l_{n+1}$$

- Incremental equation of motion:

linearized

$$m\Delta\hat{\ddot{x}}_n + c\Delta\dot{x}_{n-\alpha_f} = \Delta f_{n-\alpha_f} - \Delta r_{n-\alpha_f} = \Delta f_{n-\alpha_f} - k_t\Delta x_{n-\alpha_f} = \Delta l_n$$

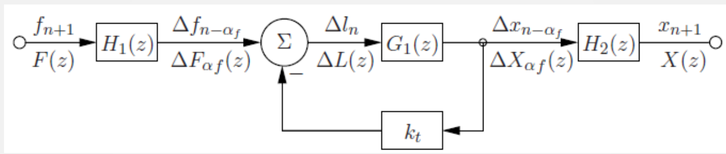

- Closed-loop transfer function:

$$G_{CL}^{NL}(z) = \frac{X(z)}{F(z)} = H_1(z)\frac{G_1(z)}{1 + k_t G_1(z)}H_2(z) = \frac{H(z)G'(z)}{1 + k_t H(z)G'(z)}$$

- $G'(z)$ is a function of α_1, α_2, and α_3, which are based on the initial stiffness (k) of the system

Kolay, C., and J.M. Ricles, "Improved Explicit Integration Algorithms for Structural Dynamic Analysis with Unconditional Stability and Controllable Numerical Dissipation," *Journal of Earthquake Engineering*, 23(5), pp 771-792, http://dx.doi.org/10.1080/13632469.2017.1326423, 2019.

Numerical Stability: Nonlinear SDOF Systems

- Study location of closed-loop poles $G_{CL}^{NL}(z)$ in complex z-plane
- Ω_{crit}= critical value of Ω below which closed-loop poles lie on or inside unit circle
  - $\Omega = \omega\Delta t$, ω = initial elastic frequency of system
- Study variation of Ω_{crit} with ratio of tangent and initial stiffness $\left(\frac{k_t}{k}\right)$ for various values of ρ_∞^*
- Closed-form expressions for stability conditions associated with $\frac{k_t}{k}$ are derived (not presented)

Kolay, C., and J.M. Ricles, "Improved Explicit Integration Algorithms for Structural Dynamic Analysis with Unconditional Stability and Controllable Numerical Dissipation," *Journal of Earthquake Engineering*, 23(5), pp 771-792, http://dx.doi.org/10.1080/13632469.2017.1326423, 2019.

Numerical Stability: Nonlinear SDOF Systems

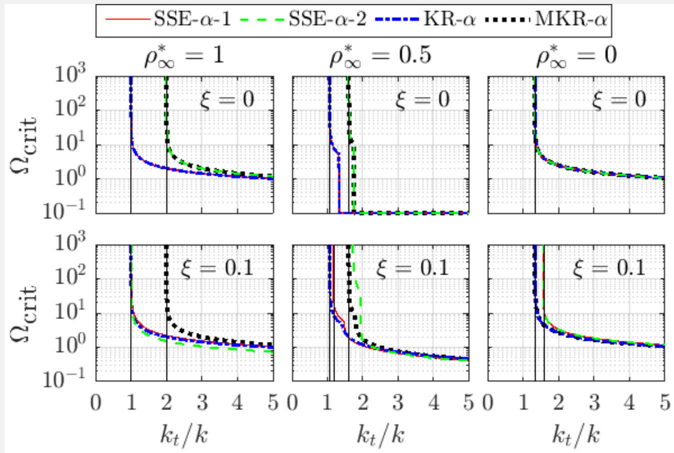

- ❑ Proposed methods are unconditionally stable within the time step for linear and stiffness softening-type ($k_t \leq \eta k$, $\eta \geq 1$) response
- ❑ MKR-α compared with KR-α and SSE-α-2 (with $\xi = 0$; $\xi \neq 0$ & $\rho_\infty^* < 1$) compared with SSE-α-1 show enhanced stability

Numerical Stability: Nonlinear MDOF Systems

- ❑ Linearized stability analysis using discrete control theory can be extended to MDOF systems
  - ➢ Transfer function becomes a matrix of transfer functions
  - ➢ Does not lead to any closed-form expression for stability conditions
- ❑ Employ linearized stability concept using energy method (Hughes et al. 1979; Hughes 1983)
  - ➢ Consider nondissipative algorithms of proposed methods

Kolay, C., and J.M. Ricles, "Improved Explicit Integration Algorithms for Structural Dynamic Analysis with Unconditional Stability and Controllable Numerical Dissipation," *Journal of Earthquake Engineering*, 23(5), pp 771-792, http://dx.doi.org/10.1080/13632469.2017.1326423, 2019.

Computational Efficiency of MKR-α Algorithm

Application to Collapse Simulation: Column Removal

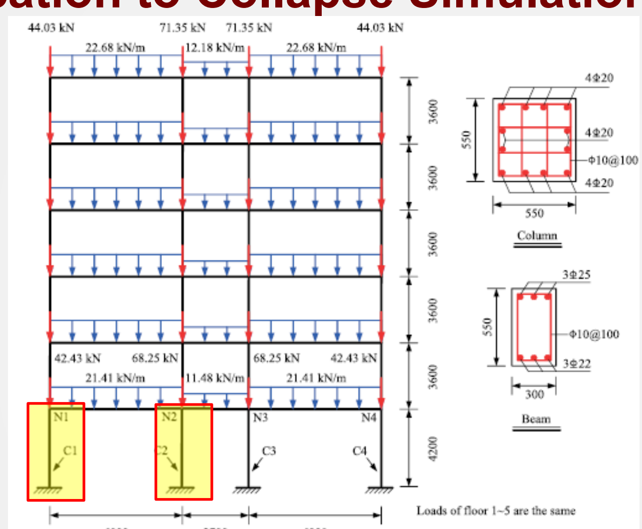

- ❑ Analysis case-1: Remove only column C2
- ❑ Analysis case-2: Remove only column C1
- ❑ Analysis performed using KR-α method
- ❑ $\Delta t = 0.001$ sec

Feng, D., Kolay, C., Ricles, J., & Li, J. (2015). Collapse simulation of reinforced concrete frame structures. *The Structural Design of Tall and Special Buildings*, (2015). doi:10.1002/tal.1273

Application to Collapse Simulation: Column Removal

Vertical displacement at N2 after removal of interior column C2

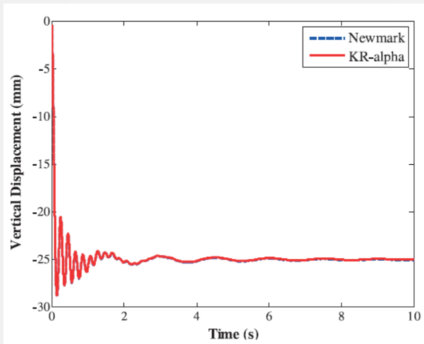

Vertical displacement at N1 after removal of exterior column C1

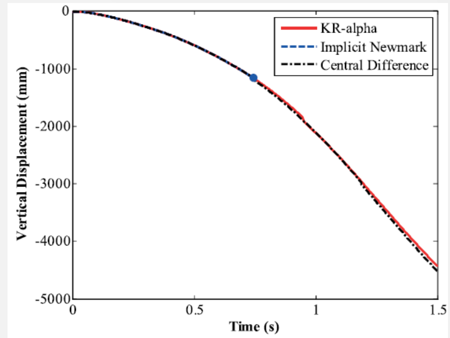

Method	Computational time (s)
Newmark CAA	208
KR-α	188

Method	Computational time (s)
Newmark CAA	-
KR-α	16
Central difference	>36,000

Feng, D., Kolay, C., Ricles, J., & Li, J. (2015). Collapse simulation of reinforced concrete frame structures. *The Structural Design of Tall and Special Buildings*, (2015). doi:10.1002/tal.1273

Seismic Collapse Simulation

1584 DOFs

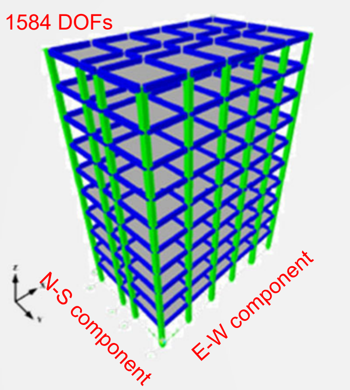

1994 Imperial Valley Earthquake scaled to 0.9 g

Computational time (s)

Method	t = 25 s	t = 28 s
Newmark CAA	668	-
KR-α	294	344

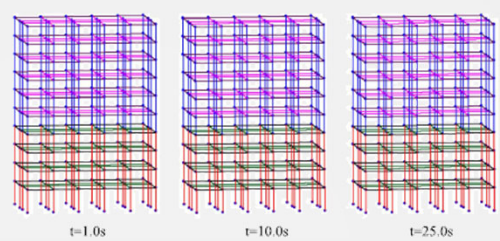

Newmark constant average acceleration: $\Delta t = 0.005$ s

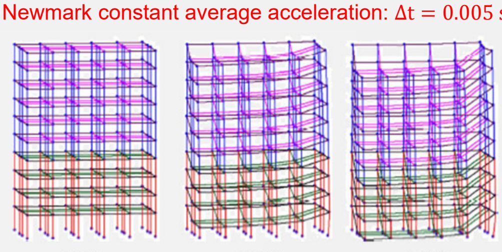

KR-α: $\Delta t = 0.005$ s & $\rho_\infty = 0.25$

Feng, D., Kolay, C., Ricles, J., & Li, J. (2015). Collapse simulation of reinforced concrete frame structures. *The Structural Design of Tall and Special Buildings*, (2015). doi:10.1002/tal.1273

Analytical Substructure Modeling

Analytical Substructure

- Desirable Characteristics of State Determination for RTHS

- Fast and accurate state determination procedure

Solution

- Explicit formulated force-based element

Fiber Element

FE Modeling of Analytical Substructure

Displacement-based fiber elements	Force-based fiber elements
❑ Curvature varies linearly	❑ Equilibrium is strictly enforced
➢ Requires many elements per structural member to model nonlinear response	✓ Material nonlinearity can be modeled using a single element per structural member
➢ Increases number of DOFs	✓ Reduces number of DOFs
❑ State determination is straight forward	❑ Requires iterations at the element level

- Must be completed within the time step
- Jeopardizes explicit integration

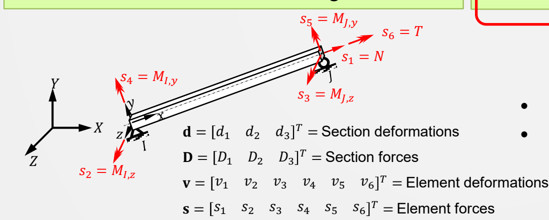

Fiber element

Force-Based Fiber Element State Determination

- ❑ Given element deformations $\mathbf{v}$, need element restoring forces $\mathbf{s}$
- ❑ Know the force interpolation function, $\mathbf{b}(x)$
  - ➢ Constant axial force and linear bending moment if no element loads
- ❑ Possible to get section forces but not clear how to get element restoring forces from section forces

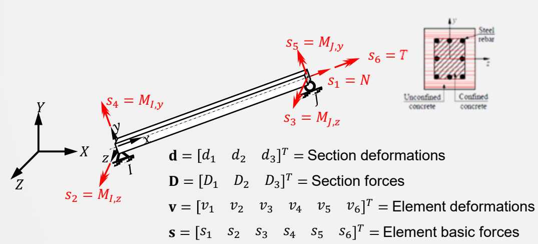

3D Explicit-Formulated Fiber Element

- ❑ Spacone et al. (1996) developed an iterative procedure at element level
  - ➢ Not well suited for RTHS
- ❑ Neuenhofer and Filippou (1997) proposed a noniterative procedure
  - ➢ Uses iteration at the structure level (Newton-Raphson type)
  - ➢ Not applicable for RTHS using explicit algorithms
- ❑ New implementation scheme
  - ➢ Limit number of iterations to a fixed value
  - ➢ Carry unbalanced section forces to the next integration time step

New Implementation Scheme

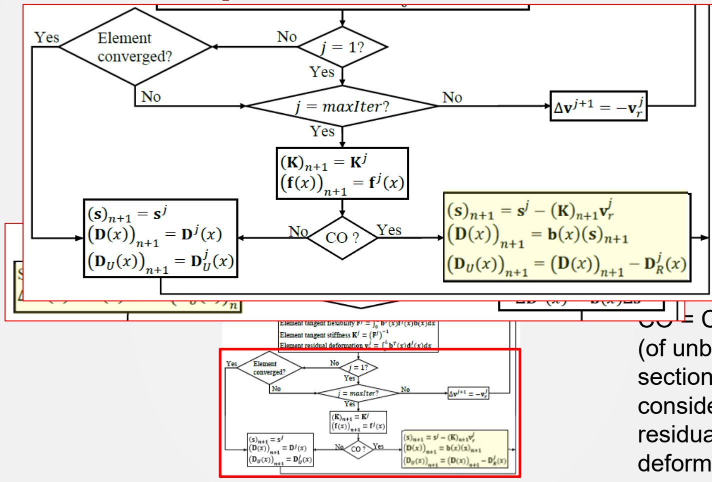

inistic
at element
satisfy
t local
ium and
ibility at
t ends

= Carry over (of unbalanced section forces, considering residual element deformations)

Kolay, C., and J.M. Ricles. (2018) "Force-Based Frame Element Implementation for Real-Time Hybrid Simulation using Explicit Direct Integration Algorithms," Journal of Structural Engineering, 144(2), https://doi.org/10.1061/(ASCE)ST.1943-541X.0001944.

Element Convergence Criteria

- ❑ Employ energy-based criteria (Taucer et al., 1991)

$$(NEI^j)_{n+1} = \frac{(EI^j)_{n+1}}{(EI^{j=1})_{n+1}} \le Etol \quad \text{for } j > 1$$

where

$$(EI^j)_{n+1} = (\Delta s^j)^T (\Delta v^j) = (\Delta v_r^{j-1})^T K^{j-1} (\Delta v_r^{j-1})$$

$$(EI^{j=1})_{n+1} = (\Delta s^{j=1})^T (\Delta v^{j=1}) = ((\Delta v)_{n+1})^T (K)_n (\Delta v)_{n+1}$$

- ❑ A typical value for $Etol = 10^{-16}$ is used (Taucer et al., 1991)

Kolay, C., and J.M. Ricles. (2018) "Force-Based Frame Element Implementation for Real-Time Hybrid Simulation using Explicit Direct Integration Algorithms," Journal of Structural Engineering, 144(2), https://doi.org/10.1061/(ASCE)ST.1943-541X.0001944.

EQ RTHS of RC Structure: Fiber Element Real-time State-Determination

Analytical Substructure: Nonlinear Explicit Force-based Fiber Elements

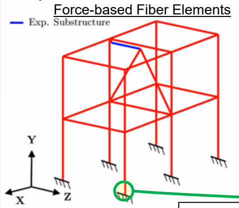

Experimental Substructure: NL Viscous Damper

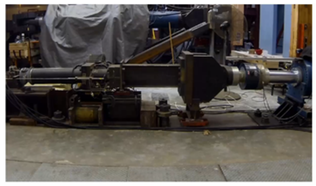

Material Constitutive Behavior

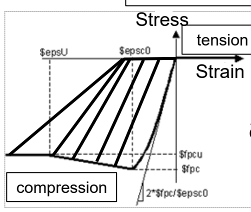

Concrete

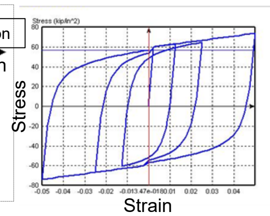

Steel Rebar

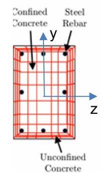

Column Cross-Section w/ 108 fibers
5 Integration Stations per Element

3D EQ Real-Time Hybrid Simulation - 2-Story R/C Building
1994 Northridge EQ, RSN960 Canyon Country Station, MCE Level

Kolay, C., and J.M. Ricles, (2018). "Force-Based Frame Element Implementation for Real-Time Hybrid Sim Integration Algorithms," *Journal of Structural Engineering*, 144(2), https://doi.org/10.1061/(ASCE)ST.19

Column develops inelastic behavior with cyclic strength and stiffness deterioration, and hysteretic pinching in force-deformation response

Explicit-formulated Force-Based Fiber Element

- Energy Error and Section Force-Deformation Results

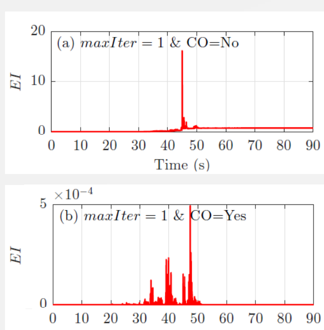

Time step Energy Increment (EI) Error – 5x10^5 times smaller

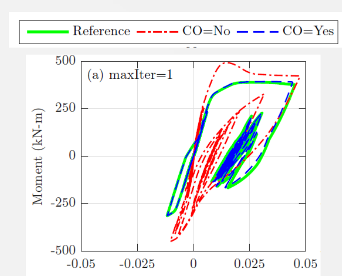

Moment Curvature Response – 1st story RC column (CO: Carry over unbalanced section forces)

Note: Reference = Newmark Constant Acceleration Method

Kolay, C. and J.M. Ricles, (2018). Force-Based Frame Element Implementation for Real-Time Hybrid Simulation Using Explicit Direct Integration Algorithms. *Journal of Structural Engineering*, 144(2) https://doi.org/10.1061/(ASCE)ST.1943-541X.0001944.

Experimental Substructure: Real-time Actuator Control

Experimental Substructure

- Desirable Servo-hydraulic Controlled System for RTHS

- Large capacity hydraulic system and dynamic actuators required
- Actuator kinematic compensation
- Robust control of dynamic actuators for large-scale structures

Solutions

Adaptive control for large servo-hydraulic actuator systems with kinematic compensation

RTHS: Experimental Substructure – Actuator Control

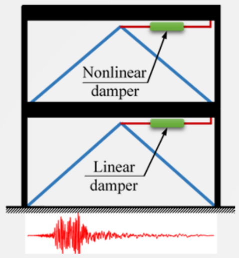

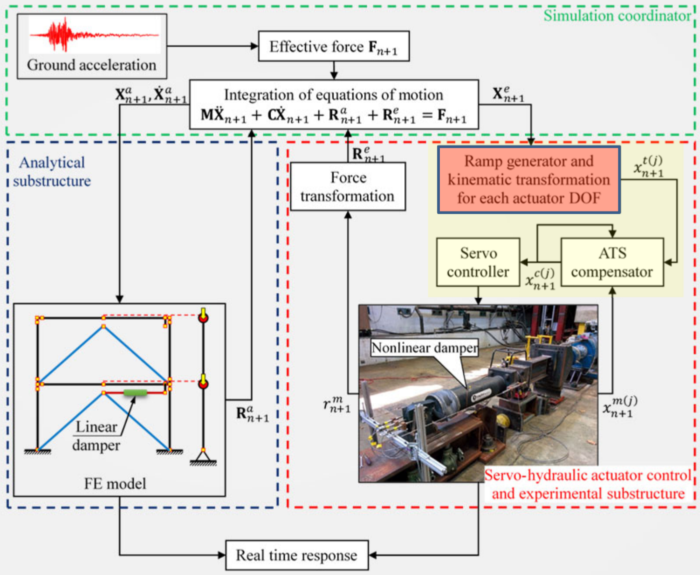

X^e_{n+1} : displacement command at time t_{n+1}, derived from integration algorithm

$x^{t(j)}_{n+1}$: actuator displacement at time t_{n+1}, derived from kinematic transformation

$x^{c(j)}_{n+1}$: compensated actuator input displacement at time t_{n+1}

$x^{m(j)}_{n+1}$: measured actuator input displacement at time t_{n+1}

LEHIGH UNIVERSITY | ATLSS | RTMD | NSF 75 YEARS OF DISCOVERY & INNOVATION | NSF NHERI CYBER-PHYSICAL SIMULATION

Actuator Kinematic Compensation: Specimen Large Target Multi-directional Displacements

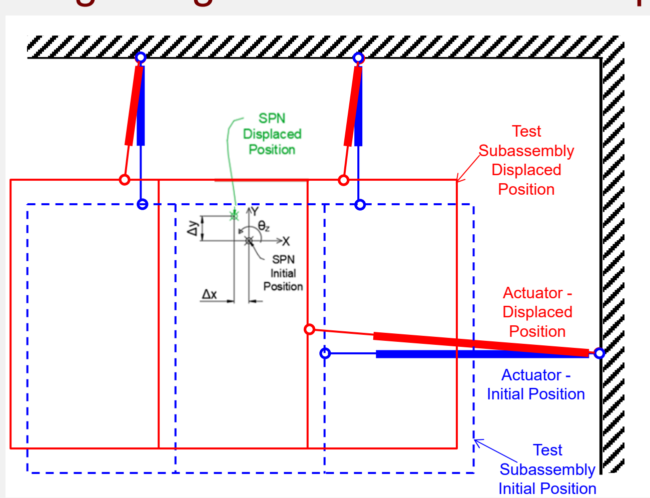

To achieve specimen’s target displaced position requires accounting for kinematic relationship between actuator DOF and specimen DOFs

Floor diaphragm subjected to in-plane bi-directional displacements

LEHIGH UNIVERSITY | ATLSS | RTMD | NSF 75 YEARS OF DISCOVERY & INNOVATION | NSF NHERI CYBER-PHYSICAL SIMULATION

Actuator Kinematic Compensation

- Kinematic compensation scheme and implementation for RTHS (Mercan et al. 2009)
  - Kinematic correction of command displacements for multi-directional actuator motions
  - Robust, avoiding accumulation of error over multiple time steps; suited for RTHS
  - Exact solution

$$(M_i SNxL_{new}, M_i SNyL_{new}) = (-LMa_{inew} sin(\Theta_2 + \phi_i), LMa_{inew} cos(\Theta_2 + \phi_i))$$

$$\Theta_2 = \arcsin\left[\frac{LMb_{inew}}{yF_i / cos\phi_i} \sin \Theta_3\right]$$

$$\Theta_3 = \arccos\left[\frac{LMa_{inew}^2 + LMb_{inew}^2 - (yF_i / cos\phi_i)^2}{2LMa_{inew} LMb_{inew}}\right]$$

$$(SPN^m x_{new}, SPN^m y_{new}) = (M_1 SN^m x_{new} - \left|\overrightarrow{VM}_1\right| cos(\Theta M_{1,0} + d^m SPN\Theta), M_1 SN^m y_{new} - \left|\overrightarrow{VM}_1\right| sin(\Theta M_{1,0} + d^m SPN\Theta))$$

Mercan, O., Ricles, J.M., Sause, R, and T. Marullo, (2009). "Kinematic Transformations in Multi-directional Pseudo-Dynamic Testing," Earthquake Engineering and Structural Dynamics, Vol. 38(9), pp. 1093-1119.

Amer, A. (2023) "Multidirectional Experimental Performance of a Seismically Resilient Self-Centering Cross-Laminated Timber Shear Wall System." PhD Dissertation, Lehigh University, Bethlehem, PA.

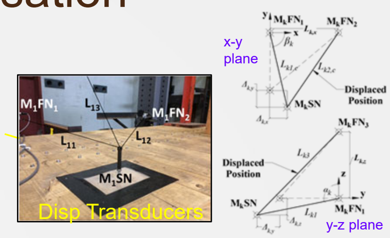

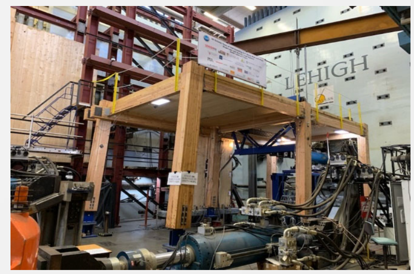

3-D motion of test sub-assembly

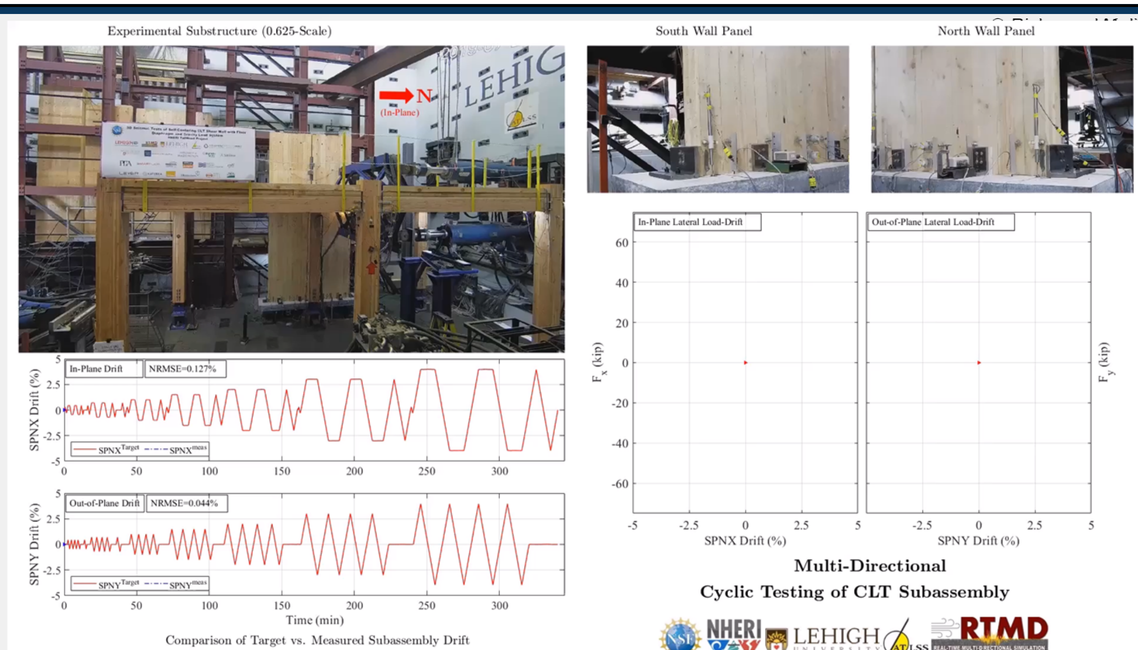

RTHS: Experimental Substructure – Actuator Control

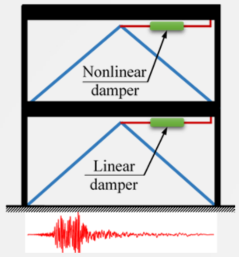

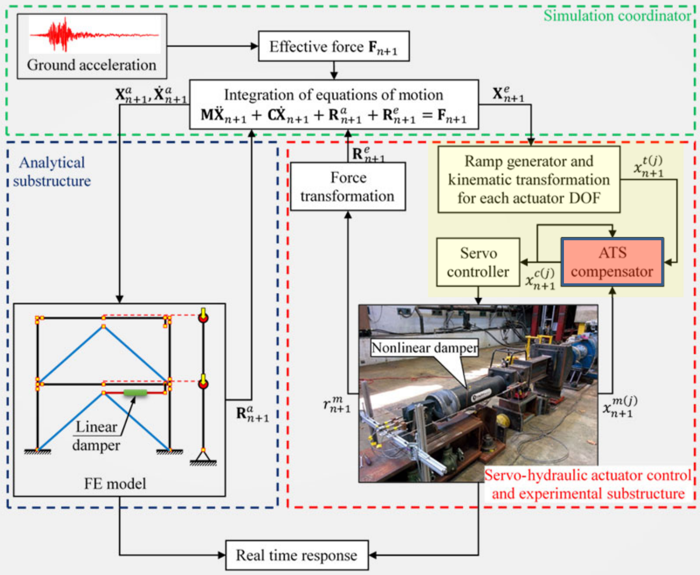

X^e_{n+1} : displacement command at time t_{n+1}, derived from integration algorithm

$x^{t(j)}_{n+1}$: actuator displacement at time t_{n+1}, derived from kinematic transformation

$x^{c(j)}_{n+1}$: compensated actuator input displacement at time t_{n+1}

$x^{m(j)}_{n+1}$: measured actuator input displacement at time t_{n+1}

LEHIGH UNIVERSITY | ATLSS | RTMD | NSF 75 | NSF NHERI CYBER-PHYSICAL SIMULATION

Dynamic Servo Hydraulic Actuator Control

Sources of Nonlinearity in Real-Time Hybrid Simulation

- Nonlinear actuator fluid and servo-valve dynamics
- Test specimen material and geometric nonlinearities
- Slop, misalignment, deformations in test setup

Can lead to variable amplitude error and time delay in servo-hydraulic system that can compromise the ability for target displacements of the experimental substructure to be achieved

Effect of time delay on real-time hybrid simulation

- Inaccurate structural response
- Delayed restoring force adds energy into the system (negative damping)
- Can cause an instability in simulation

→ Important to negate the time delay effect in real-time hybrid simulation

LEHIGH UNIVERSITY | ATLSS | RTMD | NSF 75 | NSF NHERI CYBER-PHYSICAL SIMULATION

JR [2]1

Servo Hydraulic Actuator Control
Adaptive Time Series (ATS) Compensator

Consider output displacement x of a servo-hydraulic system, with a constant time delay of τ and amplitude error A with respect to the input displacement of the actuator u at time t:

$$u(t) = \frac{1}{A} x(t+\tau)$$

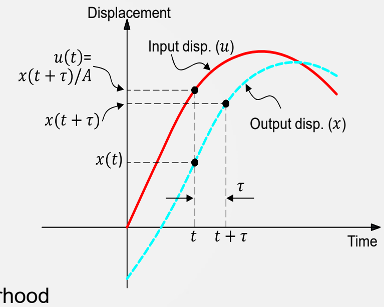

Approximate using a Taylor Series expansion, assuming x is n-times differential in the neighborhood of t:

$$u(t) \cong \frac{1}{A}\left[x(t) + \tau\dot{x}(t) + \frac{\tau^2}{2}\ddot{x}(t) + \cdots + \frac{\tau^n}{n!}\frac{d^n x}{dt^n}\right]$$

Chae, Y., Kazemibidokhti, K., and Ricles, J.M. (2013). Adaptive Time Series Compensator for Delay Compensation of Servo-hydraulic Actuator Systems for Real-time Hybrid Simulation. *Earthquake Engineering and Structural Dynamics*, 42(11), 1697-1715, DOI: 10.1002/ eqe.2294.

© Ricles and Malik, 2025

Servo Hydraulic Actuator Control
Adaptive Time Series (ATS) Compensator

To obtain accurate experimental results in a RTHS, the time delay and amplitude error need to be appropriately compensated whereby the target displacement x^t is achieved by the actuator

$$u_k^c = a_{0k}x_k^t + a_{1k}\dot{x}_k^t + \cdots + a_{nk}\frac{d^n x_k^t}{dt^n}$$

where u_k^c is the compensated input displacement into actuator at time time t_k

with the coefficients equal to

$$a_j = \frac{\tau^j}{Aj!}, \qquad j = 0,1,\cdots,n$$

Chae, Y., Kazemibidokhti, K., and Ricles, J.M. (2013). Adaptive Time Series Compensator for Delay Compensation of Servo-hydraulic Actuator Systems for Real-time Hybrid Simulation. *Earthquake Engineering and Structural Dynamics*, 42(11), 1697-1715, DOI: 10.1002/ eqe.2294.

Servo Hydraulic Actuator Control
Adaptive Time Series (ATS) Compensator

Minimize a cost function to arrive at the best actuator command displacements u_k^c in each time step of a RTHS

$$J_k = \sum_{i=1}^{q} \left(u_{k-i}^c - u_{k-i}^{est}\right)^2$$

u_{k-i}^c: compensated input displacement into actuator at time t_{k-i} associated with targeted specimen motions x_{k-i}^t, $\dot{x}_{k-i}^t$, etc.

u_{k-i}^{est}: estimated compensated input actuator displacement at time t_{k-i} associated with recent history measured specimen motions x_{k-i}^m, $\dot{x}_{k-i}^m$, etc.

where

$$u_{k-i}^c = a_{0k} x_{k-i}^t + a_{1k} \dot{x}_{k-i}^t + \cdots + a_{nk} \frac{d^n x_{k-i}^t}{dt^n}$$

$$u_{k-i}^{est} = a_{0k} x_{k-i}^m + a_{1k} \dot{x}_{k-i}^m + \cdots + a_{nk} \frac{d^n x_{k-i}^m}{dt^n}$$

Determine coefficients a_{ik} using regression analysis applied to a moving window of size $q \cdot \Delta t$

Chae, Y., Kazemibidokhti, K., and Ricles, J.M. (2013). Adaptive Time Series Compensator for Delay Compensation of Servo-hydraulic Actuator Systems for Real-time Hybrid Simulation. *Earthquake Engineering and Structural Dynamics*, 42(11), 1697-1715, DOI: 10.1002/ eqe.2294.

Servo Hydraulic Actuator Control
Adaptive Time Series (ATS) Compensator

2nd order ATS compensator

$$u_k^c = a_{0k} x_k^t + a_{jk} \dot{x}_k^t + a_{2k} \ddot{x}_k^t$$

u_k^c: compensated input displacement into actuator

x_k^t: target **specimen** displacement

a_{jk}: adaptive coefficients

Adaptive coefficients are optimally updated in real time to minimize error between the **specimen target** and **measured displacements** to avoid instabilities in a RTHS

$$\mathbf{A} = \left(\mathbf{X}_m^T \mathbf{X}_m\right)^{-1} \mathbf{X}_m^T \mathbf{U}_c$$

$$\mathbf{A} = [a_{0k}\ a_{1k}\ \cdots\ a_{nk}]^T, \quad \mathbf{X_m} = \left[\mathbf{x^m}\ \dot{\mathbf{x}}^m \cdots \frac{d^n}{dt^n}(\mathbf{x^m})\right], \ \mathbf{x^m} = \left[x_{k-1}^m\ x_{k-2}^m\ \cdots\ x_{k-q}^m\right]^T$$

$$\mathbf{U_c} = \left[u_{k-1}^c\ u_{k-2}^c\ \cdots\ u_{k-q}^c\right]^T$$

ATS Compensator

Unique features of ATS compensator

- No user-defined adaptive gains ➔ applicable for large-scale structures susceptible to damage (e.g., concrete structures)
- Negates both variable time delay and variable amplitude error response
- Time delay and amplitude response factor can be easily estimated from the identified values of the coefficients

Amplitude error: $A = \frac{1}{a_{0k}}$

Time delay: $\tau = \frac{a_{1k}}{a_{0k}}$

Chae, Y., Kazemibidokhti, K., and Ricles, J.M. (2013). Adaptive Time Series Compensator for Delay Compensation of Servo-hydraulic Actuator Systems for Real-time Hybrid Simulation. *Earthquake Engineering and Structural Dynamics*, 42(11), 1697-1715, DOI: 10.1002/ eqe.2294.

Phase 2 Large-Scale Real-Time Hybrid Simulation

Experimental Substructure: MRF and Braced Frame with Dampers
(Floor Diaphragm, Gravity System, Mass, Inherent Mass in Analytical Substructure)

Actuator control: Typical MCE level test & $\rho_\infty = 0.75$

x^t : targeted specimen displacement

u^c : input command to actuator

x^m : measured specimen displacement

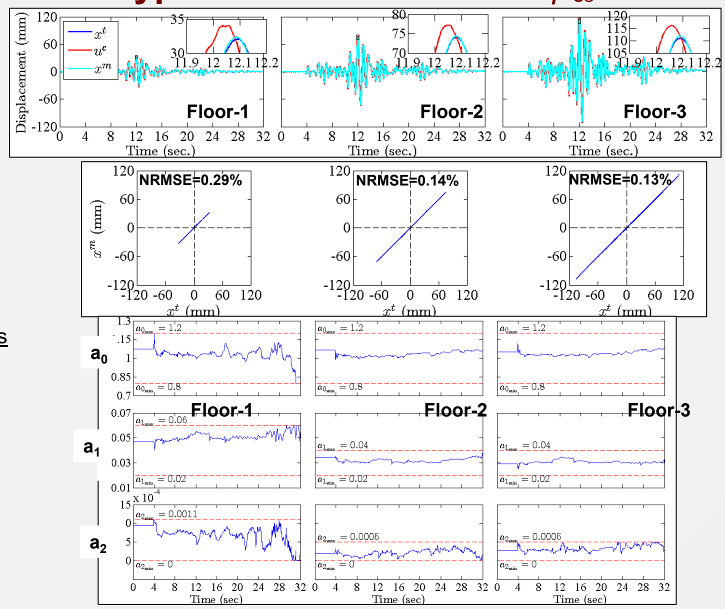

Time History of Adaptive Coefficients

Amplitude Correction

$$A_k^{(j)} \approx \frac{1}{a_{0k}^{(j)}} = 0.83 \sim 1.25$$

Delay Compensation

$$\tau_k^{(j)} \approx \frac{a_{1k}^{(j)}}{a_{0k}^{(j)}} = 18 \sim 75 \text{ msec}$$

Δt = 3/1024 sec

Analytical Substructure: On-Line Model Updating

On-line Model Updating - Motivation

- Number of physical devices in laboratory (i.e., experimental substructure) are often less than number of response modification devices in the structure
  - Accurate modeling of their complex nonlinear behavior important
  - Traditional methods for online model updating (OMU) such as Unscented Kalman Filter (UKF): sensitivity to initial parameter settings; non-positive definite covariance matrices
  - Neural networks for online model updating
- Neural networks coupled in real-time with an experimental substructure can provide optimal performance
  - **Physics based model**: Updates the parameters of the constitutive routine of the device, which is used to predict the restoring force
  - **Data-driven model**: Does not rely on a constitutive routine; directly predicts the restoring force of the device

© Ricles and Malik, 2025

Real-time Hybrid Simulation with Real-time On-line Model Updating Constrained Unscented Kalman Filter

Hybrid Wind Simulation Experiments

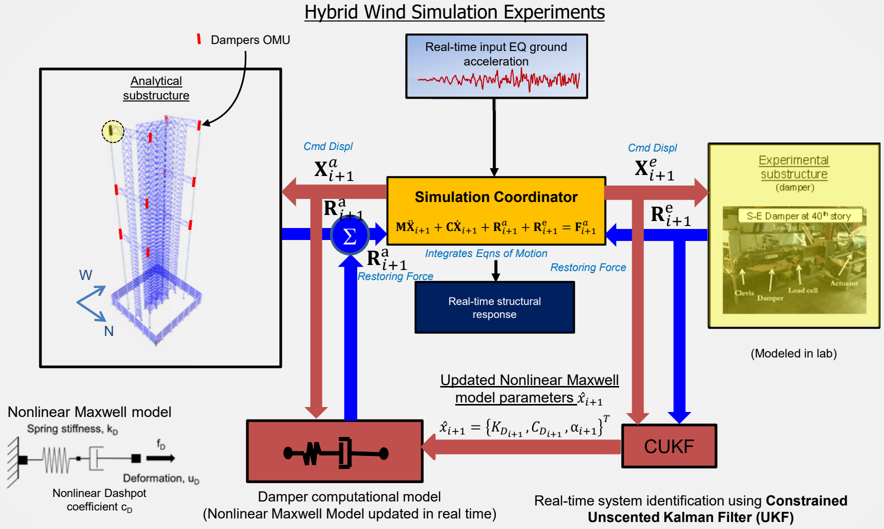

Al-Subaihawi, S., Ricles, J., and S. Quiel. "Online Explicit Model Updating of Nonlinear Viscous Damper for Real Time Hybrid Simulation," *Earthquake Engineering and Soil Dynamics*, Vol. 154, https://doi.org/10.1016/j.soildyn.2021.107108, 2022

Constrained Unscented Kalman Filter

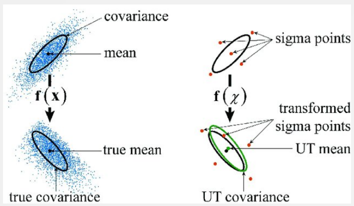

Graphical representation of the idea of UKF sigma points.

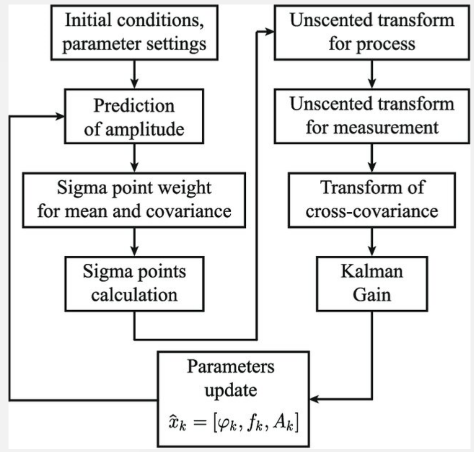

Block diagram of UKF prediction algorithm.

Wan, E. and Van Der Merwe R. The unscented Kalman filter for nonlinear estimation. In *Proceedings of the IEEE 2000 Adaptive Systems for Signal Processing, Communications, and Control Symposium*; 2000 October 1-4; Lake Louise, Alberta, Canada. DOI: 10.1109/ASSPCC.2000.882463.

Constrained Unscented Kalman Filter

Sigma points for device state variables at time step *k* of a RTHS

$$\boldsymbol{x}_{k-1|k-1} = \left[\hat{\boldsymbol{x}}_{k-1|k-1} \quad \hat{\boldsymbol{x}}_{k-1|k-1} + \left(\hat{\gamma}\sqrt{(L+\lambda)\boldsymbol{P}_{k-1|k-1}}\right)_{i=1,2,3} \quad \hat{\boldsymbol{x}}_{k-1|k-1} - \left(\hat{\gamma}\sqrt{(L+\lambda)\boldsymbol{P}_{k-1|k-1}}\right)_{i=1,2,3}\right]$$

Predicted state vector $\hat{\boldsymbol{x}}_{k|k-1}$, updated covariance matrices $\boldsymbol{P}^{xx}_{k|k-1}$ and $P^{yy}_{k|k-1}$

$$\hat{\boldsymbol{x}}_{k|k-1} = \sum_{j=0}^{2L} W_j^{(m)} * \left(\boldsymbol{x}_{k|k-1}\right)_j; \qquad \boldsymbol{P}^{xx}_{k|k-1} = \sum_{j=0}^{2L} W_j^{(c)} * \left(\left(\left(\boldsymbol{x}_{k|k-1}\right)_j - \hat{\boldsymbol{x}}_{k|k-1}\right)\left(\left(\boldsymbol{x}_{k|k-1}\right)_j - \hat{\boldsymbol{x}}_{k|k-1}\right)^T\right) + Q$$

$$P^{yy}_{k|k-1} = \sum_{j=0}^{2L} W_j^{(c)} * \left(\left(y_{k|k-1}\right)_j - \hat{y}_k\right)^2 + R$$

Prediction of the process $\hat{y}_k$ and updating of its covariance $P^{yy}_{k|k-1}$, where $h\{\cdot\}$ is the constitutive routine for the damper

$$\left(y_{k|k-1}\right)_j = h\left\{\left(\boldsymbol{x}_{k|k-1}\right)_j, \hat{y}_{k-1}, u_{d_k}, u_{d_{k-1}}, \Delta t\right\}; \qquad \hat{y}_k = \sum_{j=0}^{2L} W_j^{(m)} * \left(y_{k|k-1}\right)_j$$

$$P^{yy}_{k|k-1} = \sum_{j=0}^{2L} W_j^{(c)} * \left(\left(y_{k|k-1}\right)_j - \hat{y}_k\right)^2 + R$$

Updated state vector $\hat{\boldsymbol{x}}_{k|k}$ and covariance matrix $\boldsymbol{P}_{k|k}$, where $\bar{y}_k$ is the measured viscous damper force for the experimental substructure

$$\hat{\boldsymbol{x}}_{k|k} = \hat{\boldsymbol{x}}_{k|k-1} + \boldsymbol{K}_k\left(\bar{y}_k - \hat{y}_k\right); \qquad \boldsymbol{P}_{k|k} = \boldsymbol{P}_{k|k-1} - \boldsymbol{K}_k P^{yy}_{k|k-1}\boldsymbol{K}_k^T$$

Al-Subaihawi, S., Ricles, J., Quiel, S, and T. Marullo, "Development of Multi-directional Real-Time Hybrid Simulation for Tall Buildings Subject to Multi-natural Hazards," *Engineering Structures*, 315 (2024) 118348, https://doi.org/10.1016/j.engstruct.2024.118348, 2024

Constrained Unscented Kalman Filter: Positive Definite Covariance Matrix

Algorithm to ensure positive definite covariance $P_{k-1|k-1}$ matrix during a RTHS

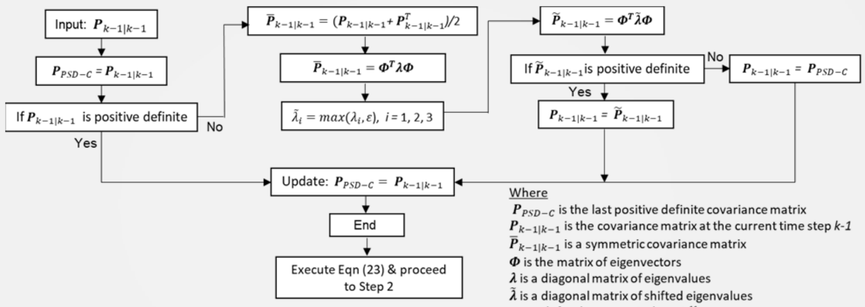

Al-Subaihawi, S., Ricles, J., Quiel, S, and T. Marullo, "Development of Multi-directional Real-Time Hybrid Simulation for Tall Buildings Subject to Multi-natural Hazards," *Engineering Structures*, 315 (2024) 118348, https://doi.org/10.1016/j.engstruct.2024.118348, 2024

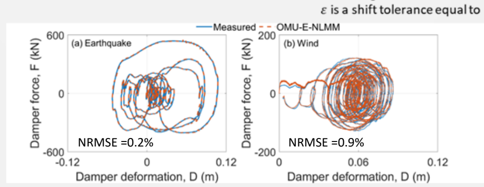

RTHS Results – Damper Model Updating Assessment Constrained Unscented Kalman Filter

Nonlinear Maxwell model

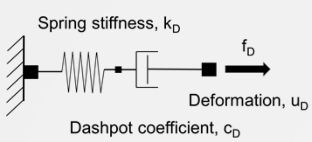

Time history of damper model parameters

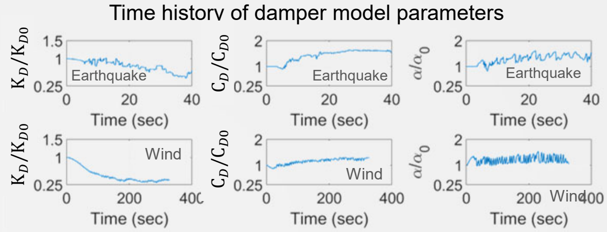

Explicit nonlinear Maxwell model formulation

$$f_{D_{k+1}} = f_{D_k} - K_D \delta t \left| \frac{f_{D_k}}{C_D} \right|^{\frac{1}{\alpha}} \text{sign}(f_{D_k}) + K_D (u_{D_{k+1}} - u_{D_k})$$

$$J_1 = \frac{|f^p - f^r|_{@f^r max}}{|f^r|_{@f^r max}} * 100, \qquad J_2 = \frac{|f^p|_{max}}{|f^r|_{max}}$$

Where:
f^p : Predicted damper force
f^r : Measured damper force
$f_{d_{k+1}}$: Damper force

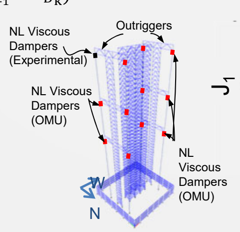

Damper error indices

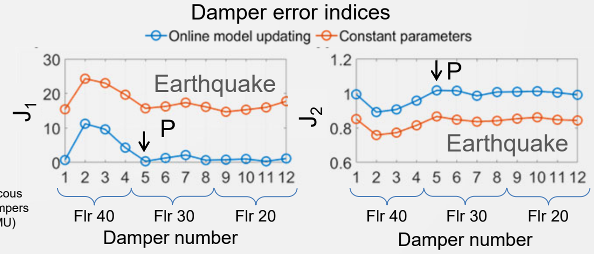

Al-Subaihawi, S., Ricles, J., and S. Quiel. "Online Explicit Model Updating of Nonlinear Viscous Damper for Real Time Hybrid Simulation," *Earthquake Engineering and Soil Dynamics*, Vol. 154, https://doi.org/10.1016/j.soildyn.2021.107108, 2022

Online Cyber-Physical Neural Network (OCP-NN) Model for RTHS

Experimental Substructure-Integrated Neural Networks (ESINN)

- Number of devices in building are often greater than the number of experimental substructures available in the laboratory.
- *In modeling the complete system, can NN models be leveraged to accurately represent the device in one location if the real-time experimental data at another location ...*

- Case Study:
  - Two story reinforced concrete SMRF used as the prototype building
  - Banded Rotary Friction Damper[1] in first story modeled physically: complex hysteretic behavior
  - Damper in second story modeled using Neural Network model

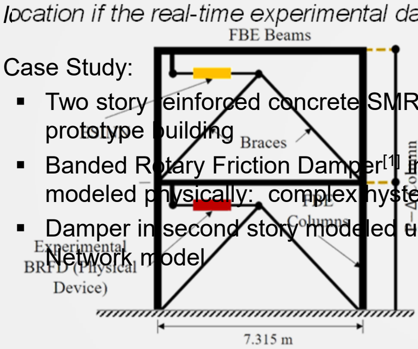

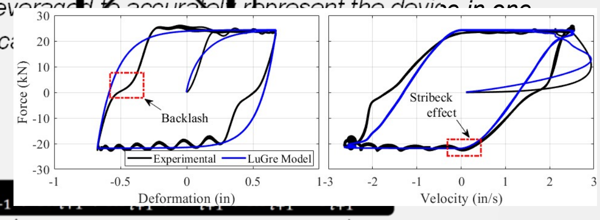

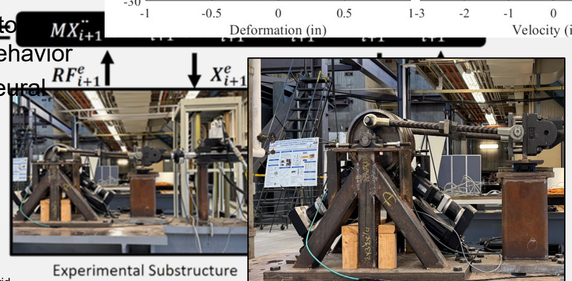

Experimental Substructure (Physical Device)

Banded Rotary Friction Device (ESINN)

[1] Cao, L., Downey, A., Laflamme, S., Taylor, D., and J. Ricles, "High Capacity Variable Friction Damper based on Band Brake Technology." *Engineering Structures*, 113 (2016) 287–298, https://DOI.org/10.1016/j.engstruct.2016.01.035, 2016.
Malik, F., Ricles, J., Cao, L., Downey, A. "Online Cyber-Physical Neural Network Model for Real-time Hybrid Simulation," *Earthquake Engineering and Structural Dynamics*, under review for publication, 2025

ESINN: Architecture, Training and Deployment

4-Layer LSTM Neural Network Architecture / Neural Network Training and Deployment

Select a suite of ground motion records

Peer NGA-west2 data

Numerical Analysis: damper deformation time histories

Experiments

Measured damper force time histories

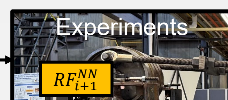

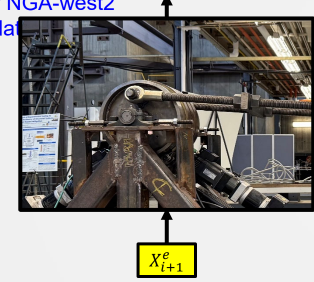

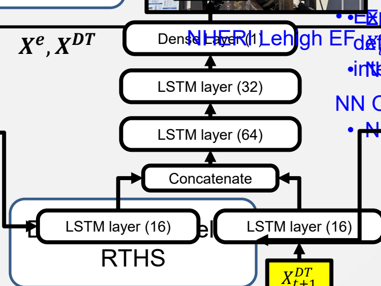

NHERI Lehigh EF

Input:
- Experimental substructure and NN model deformations X^{e}_{i+1}, X^{DT}_{i+1}
- Experimental substructure force obtained from integration

NN Output:
- NN model RF^{NN}_{i+1}

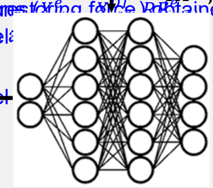

Train the NN model using TACC Frontera

Data archived on DesignSafe Data Depot

46 data set used to train and validate neural network model

Malik, F., Ricles, J., Cao, L., Downey, A. "Online Cyber-Physical Neural Network Model for Real-time Hybrid Simulation," *Earthquake Engineering and Structural Dynamics*, under review for publication, 2025.

RTHS Results: Northern Calif-03 EQ @ DBE

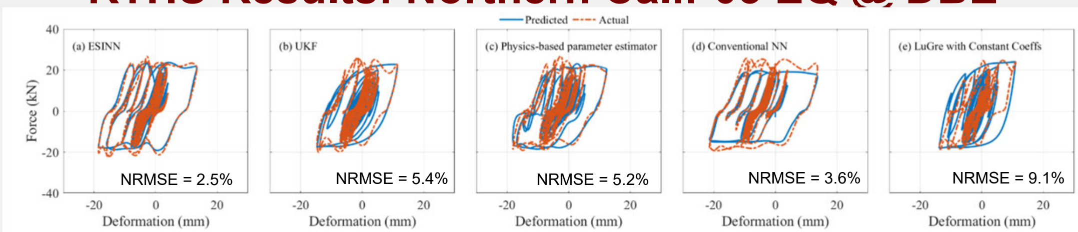

Predicted force-deformation hysteresis compared to the actual force-deformation of damper

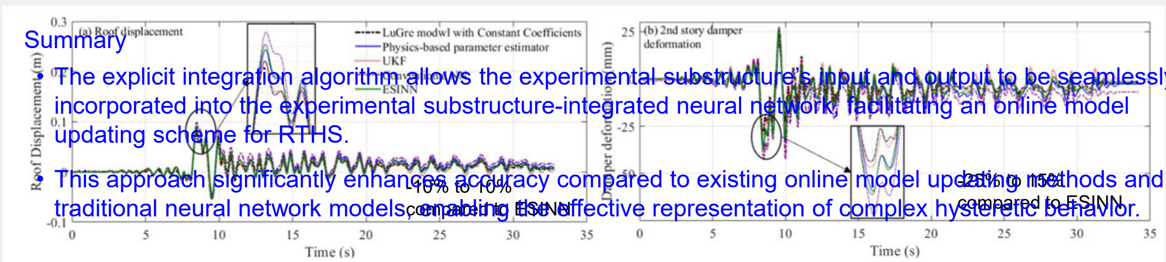

Summary

- The explicit integration algorithm allows the experimental substructure's input and output to be seamlessly incorporated into the experimental substructure-integrated neural network, facilitating an online model updating scheme for RTHS.
- This approach significantly enhances accuracy compared to existing online model updating methods and traditional neural network models, enabling the effective representation of complex hysteretic behavior.

Roof displacement response of prototype building and damper deformation

Malik, F., Ricles, J., Cao, L., Downey, A. "Online Cyber-Physical Neural Network Model for Real-time Hybrid Simulation," *Earthquake Engineering and Structural Dynamics*, under review for publication, 2025.

Real-time Hybrid Simulation: Neural Network Modeling of Multi-physics Phenomena

Why considering Soil-Foundation-Structure-Interaction is important?

- SFSI can be beneficial or determinantal to performance of structures during natural hazards
  - SFSI affects structural response during a natural hazard, such as earthquake or severe windstorm
    - Structural response; Response modification devices
- Modelling SFSI in RTHS is difficult
  - *Experimentally: Large payload size; Scaling issues*
  - *Analytically: Continuum-based modelling of soil is computationally prohibitive in real-time*

Solution: Use Neural networks to model SFSI
- *NN based models trained on continuum-based model of soil-foundation system*

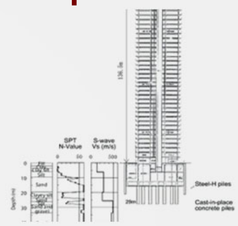

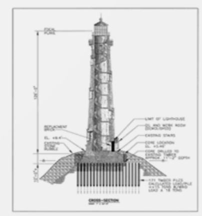

Prototype Structure

- 3-story moment resisting frame (MRF) and damped brace frame (DBF) building[1]
  - *MRF designed for strength and DBF designed to control drift*
  - *Nonlinear viscous dampers in DBF at each story level*
- Foundation designed according to Eurocode-8
- Dry sandy soil deposit calibrated to experimental data in Milan, Italy
  - *Increasing shear wave velocity with depth*

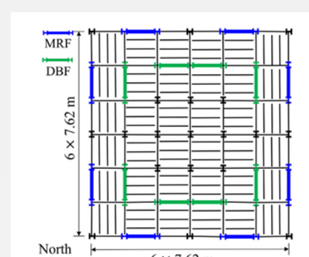

Plan

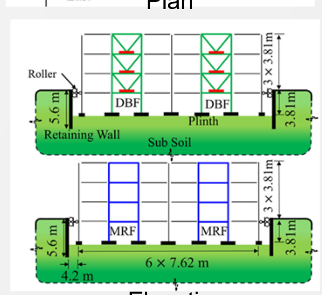

Elevation

[1] Dong, Biaping. Assessment of Nonlinear Viscous Damping Systems for Development of Seismically Resilient Structural Steel Systems, PhD Dissertation, CEE Dept., Lehigh University, 2016.
Malik, F. Gorini, D.N, Ricles, J., and M. Rahnesmoonfar, "Multi-Physics Framework for Seismic Real-time Hybrid Simulation of Soil-Foundation-Structural Systems," *Engineering Structures*, 334 (2025) 120247, https://doi.org/10.1016/j.engstruct.2025.120247, 2025.

RTHS Configuration

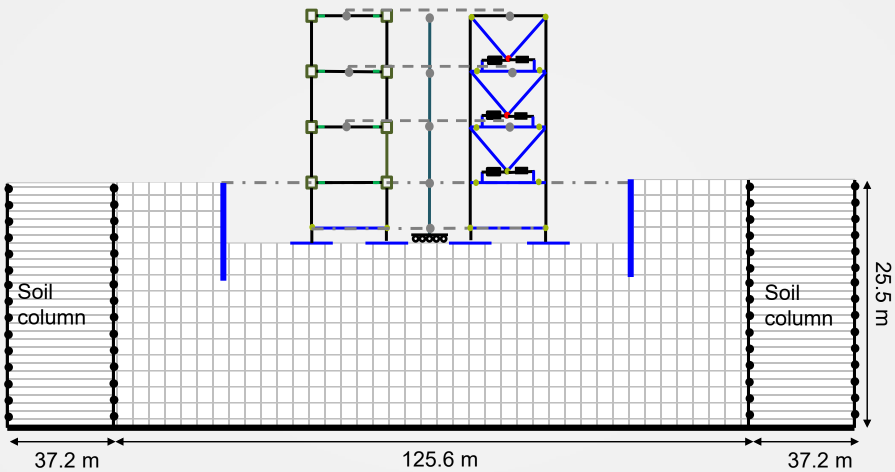

Malik, F. Gorini, D.N, Ricles, J., and M. Rahnesmoonfar, "Multi-Physics Framework for Seismic Real-time Hybrid Simulation of Soil-Foundation-Structural Systems," *Engineering Structures*, 334 (2025) 120247, https://doi.org/10.1016/j.engstruct.2025.120247, 2025.

RTHS Configuration

- Structural system divided into three substructures
  - Experimental substructure: Nonlinear viscous damper @ 3rd story
    - Manufactured by Taylor Devices
    - Physically present in the lab
  - Analytical substructure:
    - MRF and DBF without the 3rd story damper
    - 1st and 2nd story dampers using explicit nonlinear Maxwell model with real-time online model updating via a UKF[2]
    - Modeled in Simulink using HyCOM-3D[3]
  - Neural Network Substructure
    - Soil-foundation domain
    - Modeled in Simulink

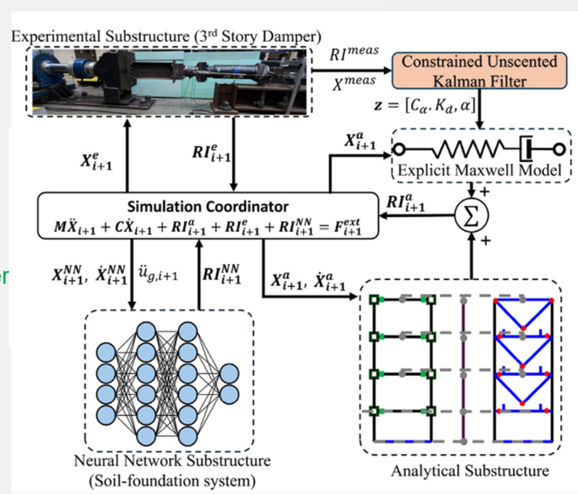

[2] Malik FN, Gorini DN, Ricles J, Rahnemoonfar M. "Multi-physics framework for seismic real-time hybrid simulation of soil–foundation–structural systems." *Engineering Structures*. 334:120247, 2025

[3] J. M. Ricles, C. Kolay, T. Marullo and F. N. Malik, "HyCoM-3D: A Program for 3D Multi-Hazard Nonlinear Analysis and Real Time Hybrid Simulation of Civil Infrastructure Systems," Version 4.2.1, ATLSS Report No. 20-02 - Appended Feb 2024, ATLSS Engineering Research Center, Lehigh University, Bethlehem, PA, 2024.

Analytical Substructure

- Columns of MRF and DBF modeled using explicit force-based fiber elements[4]
  - Steel material with kinematic hardening
- Beams of MRF modeled using FBE elements with reduced beam section flanges
  - Multiple force-based fiber elements in the MRF beams
  - RBS modeled using FBE with different section sizes at integration points
- Geometric nonlinearities accounted using lean-on P-Δ column
- Nonlinear panel zone elements at beam-to-column connections in MRF
- Beams and braces of DBF pin ended
  - Modeled using elastic beam column elements

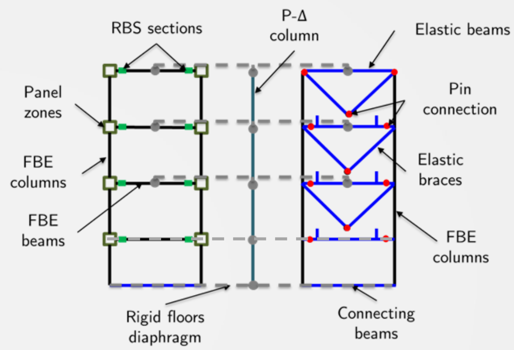

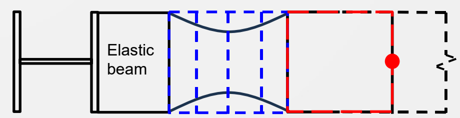

[4] C. Kolay and J. Ricles, "Force-Based Frame Element Implementation for Real-Time Hybrid Simulation Using Explicit Direct Integration Algorithms," Journal of Structural Engineering, vol. 144, no. 2, 2017.
Malik, F. Gorini, D.N, Ricles, J., and M. Rahnesmoonfar, "Multi-Physics Framework for Seismic Real-time Hybrid Simulation of Soil-Foundation-Structural Systems," *Engineering Structures*, 334 (2025) 120247, https://doi.org/10.1016/j.engstruct.2025.120247, 2025

NN Model of Soil-Foundation System

- Trained on a coupled soil-foundation-structure interaction model developed in OpenSees[5]
  - Soil elements modeled using 4 node quadrilateral type Plane Strain elements
  - Pressure Dependent Multi Yield Material model
  - Foundation modeled as an assembly of elastic beam column elements
  - Obtain interface restoring forces, displacements and velocities

[5] F. McKenna, G. Feneves and M. Scott, "Open System for Earthquake Engineering Simulation," University of California, Berkeley, Berkeley, 2000

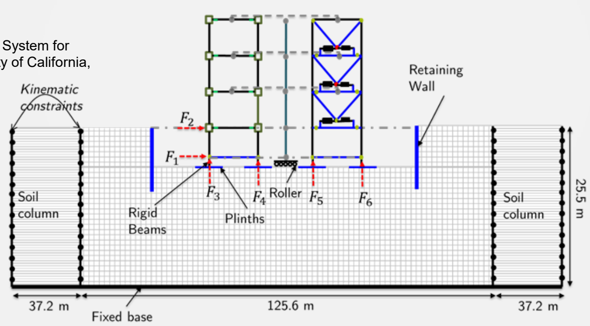

Malik, F. Gorini, D.N, Ricles, J., and M. Rahnesmoonfar, "Multi-Physics Framework for Seismic Real-time Hybrid Simulation of Soil-Foundation-Structural Systems," *Engineering Structures*, 334 (2025) 120247, https://doi.org/10.1016/j.engstruct.2025.120247, 2025.

NN Model of Soil-Foundation System (cont.)

- LSTM based NN model used to represent the soil-foundation system in RTHS
  - Parallel spring elements to eliminate rigid body modes
    - K_s is obtained by performing linear regression between interface displacements and forces
  - Parallel dashpot elements to dissipate spurious mid frequency noise

$$C_s = \frac{\int F \cdot X dx}{\int V \cdot X dx}$$

- NN model trained to predict the interface restoring force
  - Inputs: Interface displacement, velocity and ground acceleration
  - Outputs: Interface restoring forces
- Interface restoring force based on total dynamic equilibrium at the interface

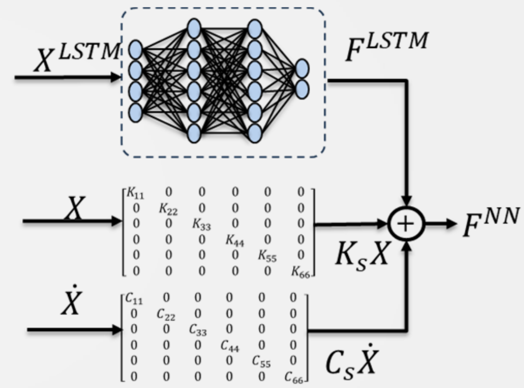

$$F_{i+1}^{NN} = F^{LSTM}(X_{i+1}, \dot{X}_{i+1}, \ddot{u}_{g,i+1}) + K_s X_{i+1} + C_s \dot{X}_{i+1}$$

X: Vector of interface displacements, $\dot{X}$ is vector of interface velocities, $\ddot{u}_g$ is the ground acceleration

NN Model of Soil-Foundation System (cont.)

- Training data generated by conducting OpenSees analysis on a suite of ground motion records
  - Ground motions obtained from PEER NGA West2 database
  - 108 records used for training the NN model
- Uncertainties in the experimental substructure properties accounted for by running OpenSees analysis with 10 different damper properties
  - Total 1080 ground motions used for training (930) and validating (150) NN model

Seismic hazard disaggregation and record selection → OpenSees SFSI model → Interface forces displacements velocities → Train the NN macroelement model → Deploy the Trained NN model in Simulink for RTHS

Malik, F. Gorini, D.N, Ricles, J., and M. Rahnesmoonfar, "Multi-Physics Framework for Seismic Real-time Hybrid Simulation of Soil-Foundation-Structural Systems," *Engineering Structures*, 334 (2025) 120247, https://doi.org/10.1016/j.engstruct.2025.120247, 2025.

NN Model of Soil-Foundation System (cont.)

- The NN model is composed of a 4-layer LSTM model
  - Adam optimizer used for gradient backpropagation
  - Regularization in the NN model to prevent overfitting
    - RTHS is closed loop; overfitting is detrimental to accuracy

LSTM-NR = Model without regularization
LSTM-DR = Model with dropout regularization

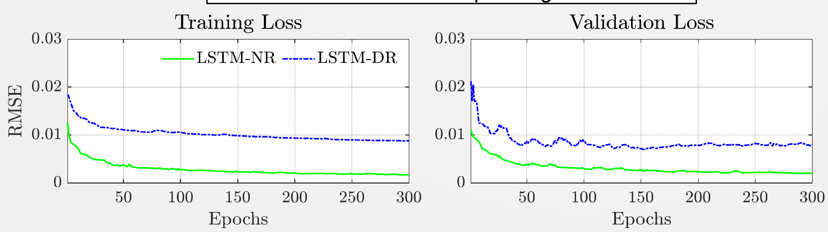

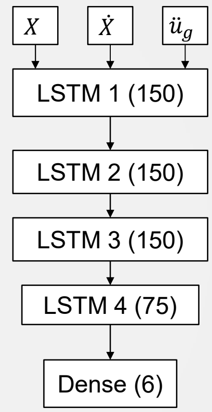

Malik, F. Gorini, D.N, Ricles, J., and M. Rahnesmoonfar, "Multi-Physics Framework for Seismic Real-time Hybrid Simulation of Soil-Foundation-Structural Systems," *Engineering Structures*, 334 (2025) 120247, https://doi.org/10.1016/j.engstruct.2025.120247, 2025.

Procedure for Analysis

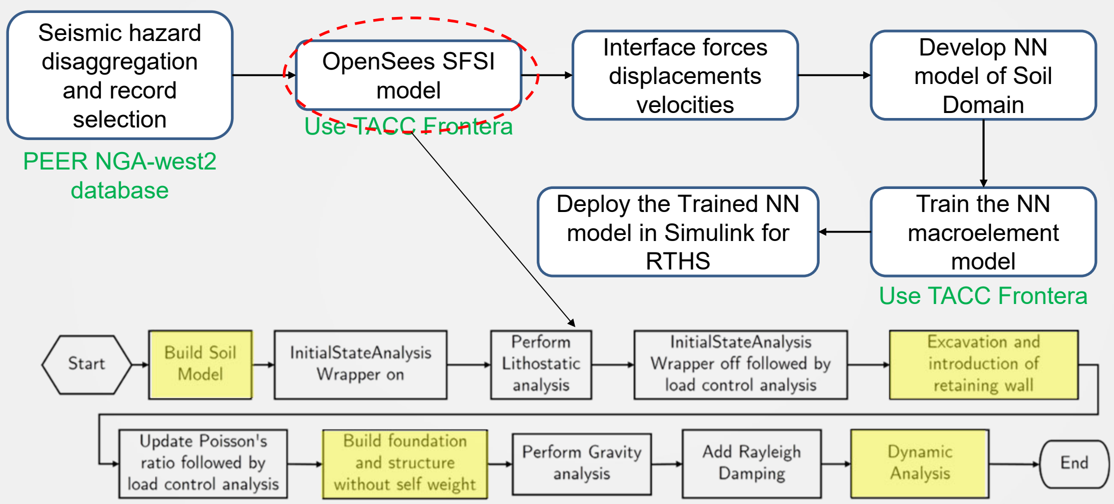

Malik, F. Gorini, D.N, Ricles, J., and M. Rahnesmoonfar, "Multi-Physics Framework for Seismic Real-time Hybrid Simulation of Soil-Foundation-Structural Systems," *Engineering Structures*, 334 (2025) 120247, https://doi.org/10.1016/j.engstruct.2025.120247, 2025.

Results: Hydraulics-off Validation

- Hydraulics-off validation conducted by using a numerical model of damper in a Simulink model
  - Linear viscous damper with damping coefficient of 3600 kNs/m
  - Same damper properties used in OpenSees model (reference solution) and compared to Simulink model

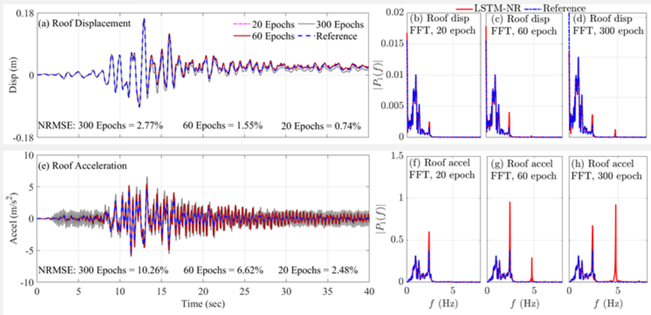

LSTM-NR: Model without regularization

Malik, F. Gorini, D.N, Ricles, J., and M. Rahnesmoonfar, "Multi-Physics Framework for Seismic Real-time Hybrid Simulation of Soil-Foundation-Structural Systems," *Engineering Structures*, 334 (2025) 120247, https://doi.org/10.1016/j.engstruct.2025.120247, 2025.

Results: Hydraulics-off Validation

- Hydraulics-off validation conducted by using a numerical model of damper in the Simulink model
  - Linear viscous damper with damping coefficient of 3600 kNs/m
  - Same damper properties used in OpenSees model (reference solution) and compared to Simulink model

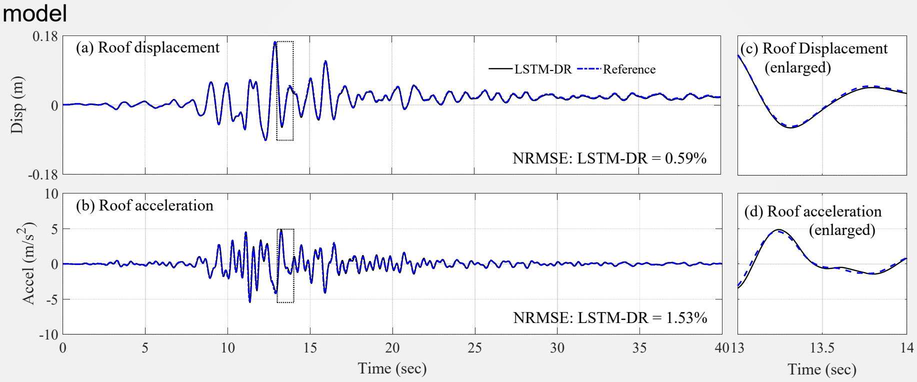

LSTM-DR: Model with regularization

Malik, F. Gorini, D.N, Ricles, J., and M. Rahnesmoonfar, "Multi-Physics Framework for Seismic Real-time Hybrid Simulation of Soil-Foundation-Structural Systems," *Engineering Structures*, 334 (2025) 120247, https://doi.org/10.1016/j.engstruct.2025.120247, 2025.

Results: Hydraulics-off Validation

- Hydraulics-off validation conducted by using a numerical model of damper in the Simulink model
  - Linear viscous damper with damping coefficient of 3600 kNs/m
  - Same damper properties used in OpenSees model (reference solution) and compared to Simulink model

NRMSE (%) on the hydraulics-off validation dataset

Response	LSTM-NR (20 epoch)	LSTM-NR (300 epoch)	LSTM-DR
Roof displacement	0.70 ± 0.33	3.51 ± 0.88	0.43 ± 0.26
Roof acceleration	2.83 ± 1.06	16.15 ± 2.72	1.88 ± 0.65
Damper deformation	1.47 ± 0.73	3.18 ± 0.70	0.77 ± 0.39

Malik, F. Gorini, D.N, Ricles, J., and M. Rahnesmoonfar, "Multi-Physics Framework for Seismic Real-time Hybrid Simulation of Soil-Foundation-Structural Systems," *Engineering Structures*, 334 (2025) 120247, https://doi.org/10.1016/j.engstruct.2025.120247, 2025.

Multi-Physics Cyber-Physical Simulation: RTHS with SFSI Effects

Relevance of Soil-Foundation-Structure Interaction (SFSI) Effects

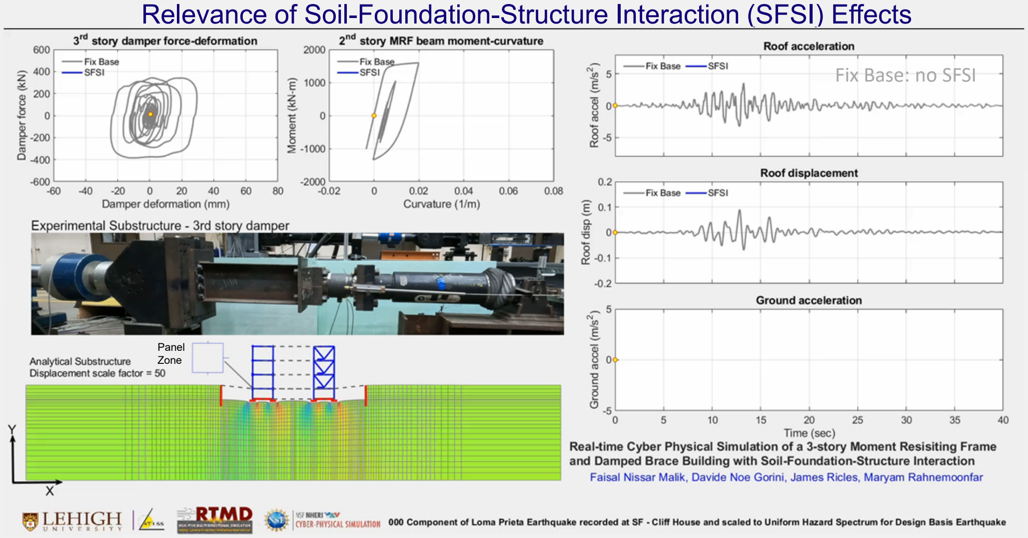

Malik, F. Gorini, D.N, Ricles, J., and M. Rahnesmoonfar, "Multi-Physics Framework for Seismic Real-time Hybrid Simulation of Soil-Foundation-Structural Systems," *Engineering Structures*, 334 (2025) 120247, https://doi.org/10.1016/j.engstruct.2025.120247, 2025.

Results: Comparison Between SFSI and Fixed Base

- Accounting for SFSI leads to
  - Increase in displacement demand of damper; Increase in peak damper force→ Higher member forces
  - Increased Ductility in structural members
  - Increased peak and residual displacements

Loma Prieta ground motion recorded at SF Cliff House

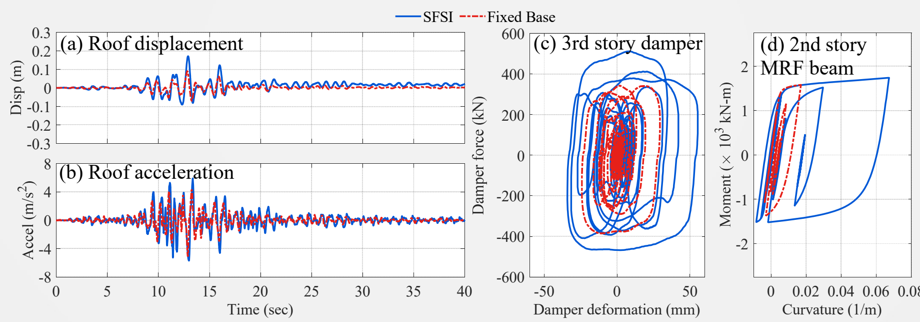

Malik, F. Gorini, D.N, Ricles, J., and M. Rahnesmoonfar, "Multi-Physics Framework for Seismic Real-time Hybrid Simulation of Soil-Foundation-Structural Systems," *Engineering Structures*, 334 (2025) 120247, https://doi.org/10.1016/j.engstruct.2025.120247, 2025.

RTHS Results: Statistics on Ensemble of 14 Ground Motions

- Ensemble of 14 ground motion records
- Accounting for SFSI leads to an increase in
  - *Peak inter-story drift: 61 %*
  - *Peak damper deformation: 65 %*
  - *Residual inter-story drift*
    - No residual inter-story drift observed in Fixed Base (i.e., no foundation) case.
    - Residual inter-story drift when SFSI is considered

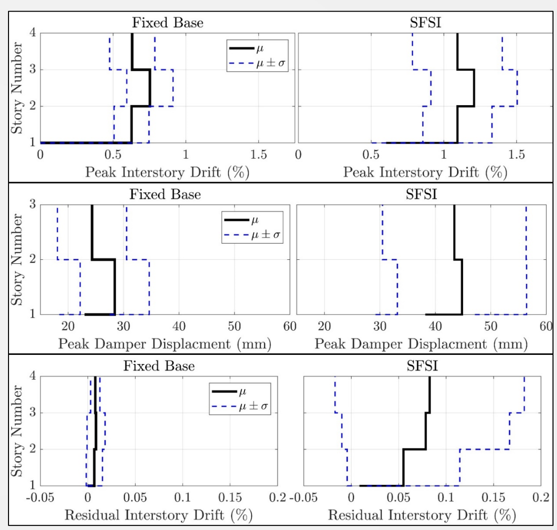

Malik, F. Gorini, D.N, Ricles, J., and M. Rahnesmoonfar, "Multi-Physics Framework for Seismic Real-time Hybrid Simulation of Soil-Foundation-Structural Systems," *Engineering Structures*, 334 (2025) 120247, https://doi.org/10.1016/j.engstruct.2025.120247, 2025.

Results: RTHS Error Quantification

- NN model restoring forces during the RTHS input to OpenSees SFSI model
  - Resulting interface displacements compared to ones obtained from RTHS

Loma Prieta ground motion recorded at Point Bonita

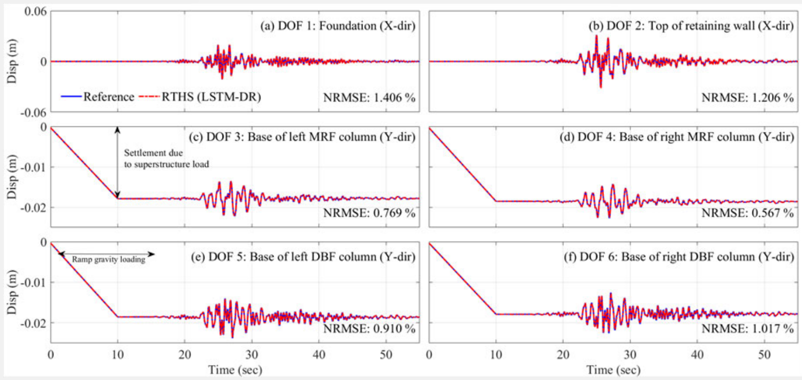

Malik, F. Gorini, D.N, Ricles, J., and M. Rahnesmoonfar, "Multi-Physics Framework for Seismic Real-time Hybrid Simulation of Soil-Foundation-Structural Systems," *Engineering Structures*, 334 (2025) 120247, https://doi.org/10.1016/j.engstruct.2025.120247, 2025.

LEHIGH UNIVERSITY | ATLSS | RTMD | NSF 75 YEARS OF DISCOVERY & INNOVATION | NSF NHERI CYBER-PHYSICAL SIMULATION